The characterisation of thin films of polyaniline for gas sensing

Margaret T. Scully

The Characterisation of Thin Films of Polyaniline for Gas Sensing

by

Margaret T. Scully

A thesis submitted to the Faculty of Science,
Durham University, for the degree of Master of Science.

Department of Physics,
University of Durham,
October 1994.

Declaration

The material contained in this thesis has not been submitted for examination for any other degree, or part thereof at the University of Durham or any other institution. The material contained in this thesis is the work of the author except where formally acknowledged by reference,

Acknowledgements

I would like to thank my two supervisors, Dr Mike Petty and Dr Andy Monkman for arranging this project and for all of the time, effort and enthusiasm they have given me throughout my time at Durham.

May I express a deep gratitude to British Gas for sponsoring this MSc project and a special thanks to Dr Mary Harris and Dr Mario Petrucci.

A big thank-you to everyone in the department, especially Norman, Chris and John (the technicians), Sharon and Julie (the secretaries) and Julie and Kay (in the drawing office) for all of their help.

My friends on Geco Tau deserve a mention, for all of their encouragement in getting me to finish this thesis!

Finally, I would like to thank Alex, mum and dad, for their patience, love and support throughout this project.

Dedication

To Dad, I miss you.

Abstract

This project is concerned with the preparation of high quality polyaniline thin films, which can be used as a gas sensor. A 5% solution of emeraldine-base polyaniline (the insulating form) was dissolved in N-methyl-2-pyrrolidinone (NMP) and left for 48 hours, before either being centrifuged three times (and decanted) or being homogenised. These methods ensured the removal of any lumps. The solution was then spun onto circular glass or sapphire substrates (which had been cleaned in isopropanol for one hour) and the spinning conditions could be altered on the programmable spinner. Thin films (the order of micrometers) were spun and the whole process was carried out in a clean room environment.

Polyaniline-coated interdigitated electrodes measured a change in resistance upon exposure to NO_x gas. Certain parameters (i.e. gas concentration, response time, recovery time) were varied and the response of three sensors (of different thickness) were noted. The results suggested that the change upon exposure was due to a surface effect and the best sensor was found to be 0.19μm thick.

Optical experiments carried out on the spun films (typically in the order of 0.2μm thick) found that at 2.7eV, the absorption coefficient of polyaniline was $1.7 \times 10^5 c\,m^{-1}$. Following on from this, certain energy levels could be measured accurately. The optical band-gap was found to be 1.47eV and also, other transitions were measured at 3.19eV and 5.56eV.

Contents

Chapter 1

Introduction

A gas sensor is a transducer which will show certain property changes when exposed to an environment that contains a particular molecular species. These property changes may then be converted into an electrical signal [1].

Although there are already several sensors available, based on semiconductor oxides [2], these are found to be unreliable. So, the general aim of this project is to develop a sensor which shows durability, improved sensitivity at low gas concentrations and selectivity to a particular gas. Other important concerns are that the sensor responds at room temperature and that once the gas is removed the sensor shows reversibility (i.e., it returns to its original state, or as near as possible, indicating that the effect of exposure to the gas is not permanent).

The gas sensor is produced by depositing a thin film of polyaniline, a polymer, onto interdigitated electrodes. Polyaniline is the oldest known synthetic conjugated organic polymer [3] and derives from the polymerisation of aniline. Polyaniline is a family of four different chemical forms:

(a) Emeraldine-salt, shown in Figure 1.1(a) is a conducting form, exhibiting values of 5 Scm^{-1} in the powder form, 70 Scm^{-1} as an 'as cast' film and 350 Scm^{-1} in films stretched and measured parallel to the stretch direction [4].

(b) Emeraldine-base, which is insulating and is semi-oxidised. From Figure 1.1(b) it can be seen that half the amine nitrogens have been oxidised to form

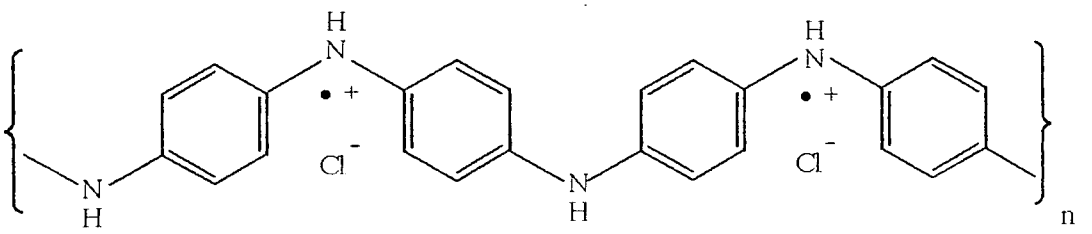

(a) Emeraldine Salt

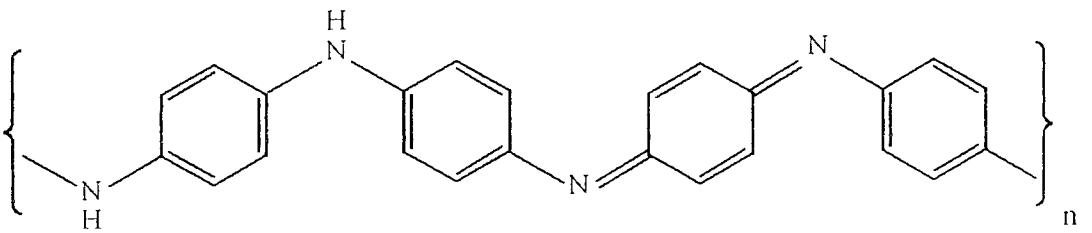

(b) Emeraldine Base

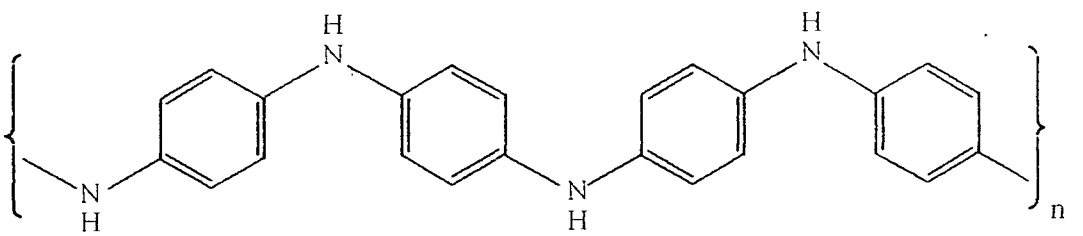

(c) Leucoemeraldine Base

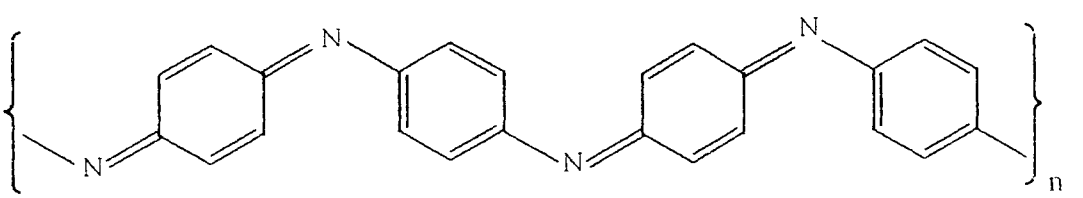

(d) Pernigraniline Base

Figure 1.1. The four chemical states of polyaniline.

imine nitrogens and these no longer carry hydrogen atoms. These oxidised and reduced 'units' alternate along the polymer chain.
(c) Leucoemeraldine-base is also insulating and fully reduced, Figure 1.1(c).
(d) Pernigraniline-base which is fully oxidised and insulating, Figure 1.1(d).

Of particular interest for this work is the emeraldine base form. Although it is an insulator, by protonating (i.e doping) with aqueous acid the base is converted to the salt (electrically conducting) form. This latter form of the polymer has a conductivity approximately ten orders of magnitude greater than that of its base derivative.

Although there are many methods with which to deposit thin films onto a substrate, such as evaporation, sputtering etc., polyaniline is deposited onto interdigitated electrodes by the spinning process. Spinning is a popular method for depositing a solution onto a substrate and a lot of work has already been carried out to investigate the effect this method has on the film [5],[6]. However, this thesis is primarily concerned with the effect spinning has on polyaniline (which has been dissolved in N-methyl-2-pyrrolidinone, NMP, to form a solution [7]). Further to the work already carried out at Durham on this topic [8], this thesis presents more results concerning the spin-coating process, its effect on thin films of polyaniline [9] and hence on the device behaviour as a gas sensor.

As a sponsor of this project, British Gas plc., was interested in carrying out research into a novel gas sensor, with the possibility of producing it on a commercial scale. It could be used to detect any hazardous gas leaks, should they occur in the pipes transporting the gas from the rig site, through to the individuals home.
The contents of each chapter are set out as follows:-

Chapter 2 is involved with the spinning process itself. The spinning conditions to produce a good thin film are investigated, as is the best

solution to work with (e.g. percentage of polyaniline by weight), the best solvent to dissolve polyaniline and also the best way to prepare the solution before it is spun (to minimise the amount of lumps, which otherwise effect the final quality of the spun-film).

Chapter 3 is concerned with the optical properties of these films. By carrying out optical measurements on samples of various thickness, the absorption coefficient of polyaniline can be calculated. From this, the optical band gap and various other energy transitions can be found.

Chapter 4 deals with gas sensing experiments. Thin films of different thickness are spun onto interdigitated electrodes and these are exposed to various concentrations of NO_x gas (which in this work is NO_2) for varying degrees of time. This sensor monitors a change in resistance on the surface of the film as this is a surface dominated effect. The time taken for the device to react (delay time), the change due to exposure to NO_x gas and the time taken for the device to recover once the gas has been removed, are all investigated. This requires monitoring the change in resistance across the thin film surface.

The final chapter, Chapter 5, concludes this work and adds suggestions for further work which could be carried out.

References

[1] P.Clechet - Sensors and Actuators B, **4**,(1991),53-63.

[2] A.Jones, T.Jones, B.Mann, J.Firth - Sensors and Actuators, **5**,(1984), 75-88.

[3] H.Lethby - J.Chem. Soc., **15**,(1862),161.

[4] A.Monkman and P.Adams - Synthetic Metals, **41-43**,(1991)627-633.

[5] P.Sukanek - J. Electrochem. Soc., No. 6, **138**,(1991),1712-1719.

[6] A.Weill and E.Dechenaux - Polymer Engineering and Science, No. 15, **28**,(1988),945-948.

[7] European Patent Application, No. 89117826.1.

[8] N.E Agbor, M.Petty, M.Scully, A.Monkman - Patent Application No. UK/9300560.1/1993.

[9] M.Scully, M.Petty - Synthetic Metals, **55-57**,(1993),183-187.

Chapter 2

The deposition of polyaniline thin films using the spin-coating technique

2.0 Introduction

Spin-coating is a common technique employed to deposit thin films of a wide variety of materials onto suitable substrates. The films must be evenly spread and lump-free and there is also a need to be able to reproduce reliable, high quality films. To date, work has been carried out on a number of polymers with regards to their behaviour to spinning [1]. However, nothing is known specifically about spun films of deprotonated emeraldine-base polyaniline. Therefore, time has been devoted to the processing of such films, enabling us to gather as much information as possible.

2.1 The Solent Semiconductor Spinner

The spinner used throughout this work was a photoresist coater (Model 4000-Solent Semiconductor services), incorporating a remote control unit and an infra-red heating lamp as shown in Figure 2.1. The instrument was capable of spinning up to 6000 revolutions per minute (rpm) and heating to 350°C. The spinner was also connected to a vacuum pump. A switch on the remote control unit controlled the vacuum, and this was necessary to keep the substrate in place. As a safeguard mechanism, the spinner would not spin unless the vacuum was switched on.

Figure 2.2 shows the key pad on the remote control unit, which could be programmed when the spinner was stationary. It was found that the

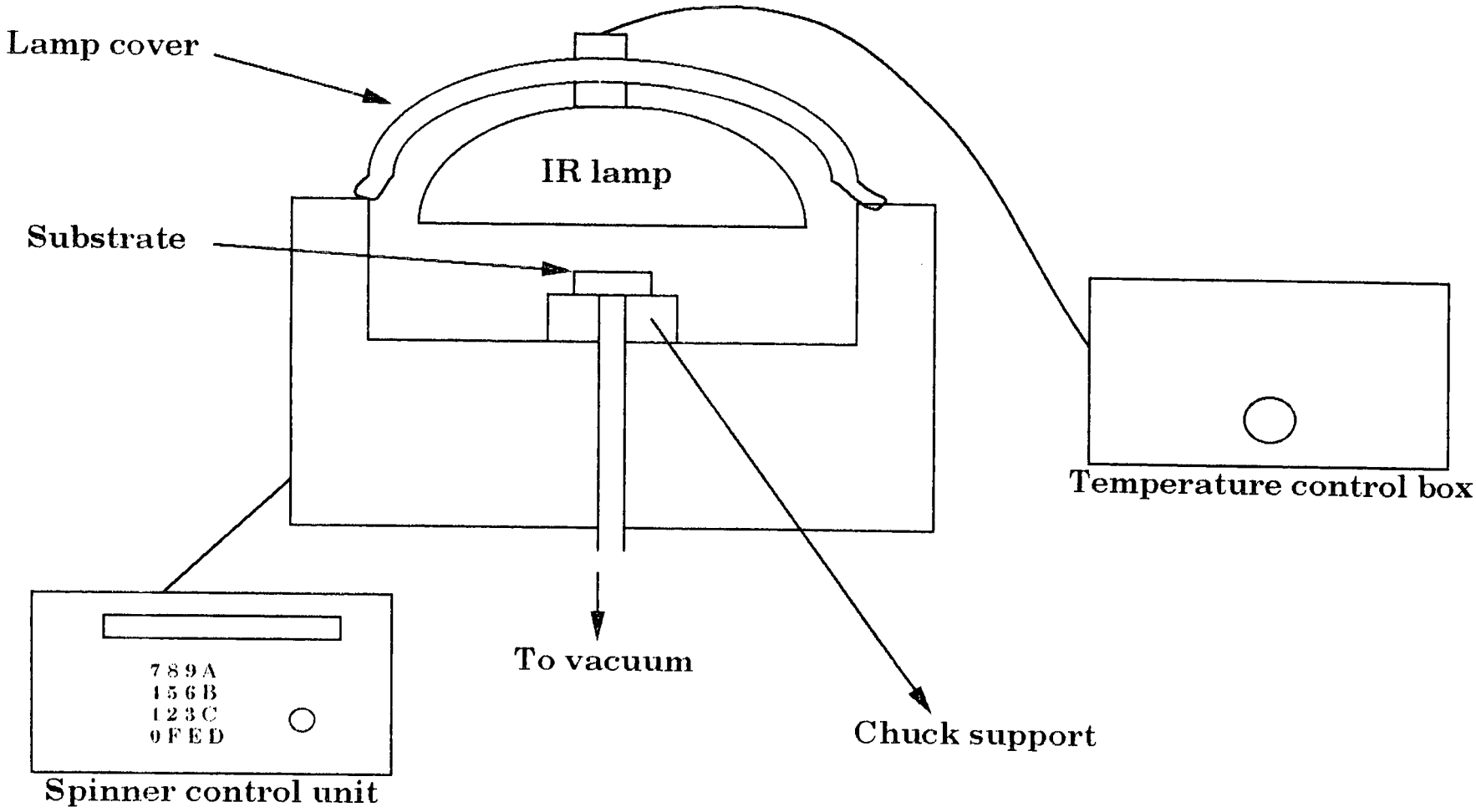

Figure 2.1. The set-up of the spinner, including the infra-red lamp and the spinner control unit.

7	8	9	A
4	5	6	B
1	2	3	C
0	F	E	D

On the spinner, the alphabetic keys have the following functions;

A = Used to enter speed. The unit responds by asking for which stage the value is required. Input speed is from 1 to 4090 units (which has been converted to rpm in Figure 3.3).

B = Used to enter time. The unit responds by asking for which stage the value is required. Input time is from 0 to 650 seconds.

C = Used to enter the ramp value. The unit responds by asking for which stage the value is required. Input values are from 1 to 256 (where the lower the value, the longer the ramp).

D = This is concerned with saving the present values which have been inputed, to be used when the unit is next powered up.

E = ENTER KEY. Required to enter each value i.e choose parameter to be changed, put in new value and then press E (enter).

F = Reserved for further use.

Figure 2.2. The layout of the key-pad on the spinner.

speed value (A) was given in arbitrary units, but was displayed on the remote control unit in rpm (revolutions per minute). To spin at a specific rpm, a calibration graph of unit speed versus rpm speed was required. For an input speed (in arbitrary units), the spinner was initiated and the displayed rpm was read off the control unit. It was assumed that the rpm display was the actual speed at which the chuck on the spinner rotated. A graph of rpm versus speed, in arbitrary units was plotted from 100rpm up to 6000rpm. This calibration curve is shown in Figure 2.3.

The ramp value (C) was another parameter, giving the acceleration/deceleration of the spinner. The lower the number chosen, the slower the acceleration/deceleration.

The remote control unit was programmable in three stages: the initial stage (builds up the speed); the spinning stage, at constant speed (when the solution on the substrate is spun); the final stage (deceleration of the substrate).This has been summarised diagrammatically in Figure 2.4.

v_1 was the maximum velocity reached for stage 1 of the process, by accelerating with a value a_1 (the time taken for this acceleration was negligible). v_1 was maintained for a time t_1 and during this stage the solution was spread homogeneously over the substrate.

v_2 was the maximum velocity reached for stage 2 of the process, by accelerating with a value a_2 (the time taken for this acceleration was negligible). v_2 was maintained for a time t_2 and during this stage any excess solution was spun off the substrate, due to the action of centrifugal forces.

v_3 was the velocity reached for stage 3, by a deceleration of value a_3. v_3 was maintained for a time t_3 after which the spinner came to a stop, by decelerating with a value a_4. This occurred over a negligible amount of time, but if a value for a_4 had not been programmed into the unit, the substrate came to an abrupt stop and was normally thrown off the spinner.

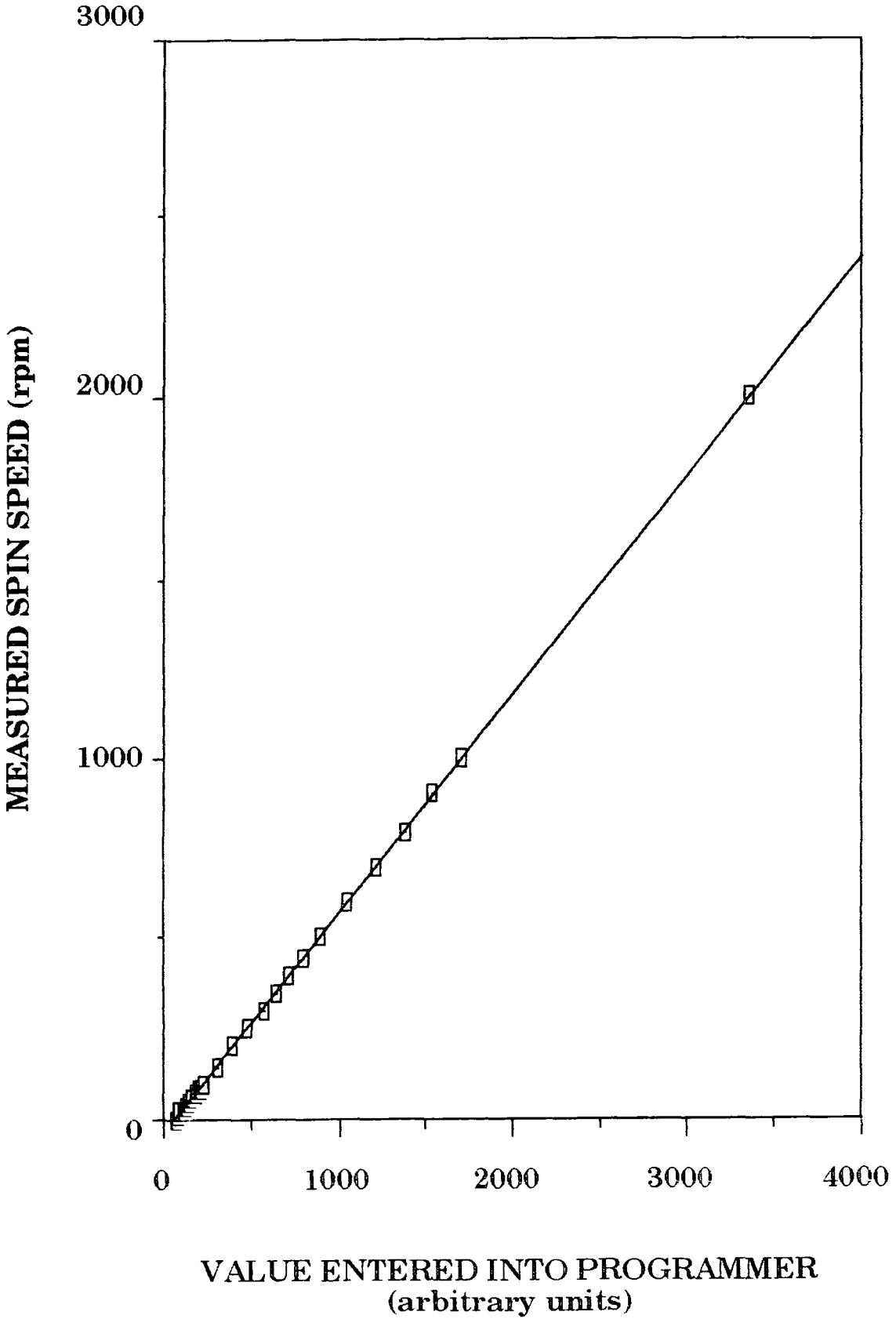

Figure 2.3. The calibration of speed (in arbitrary units) as a function of speed (in rpm), for the spinner.

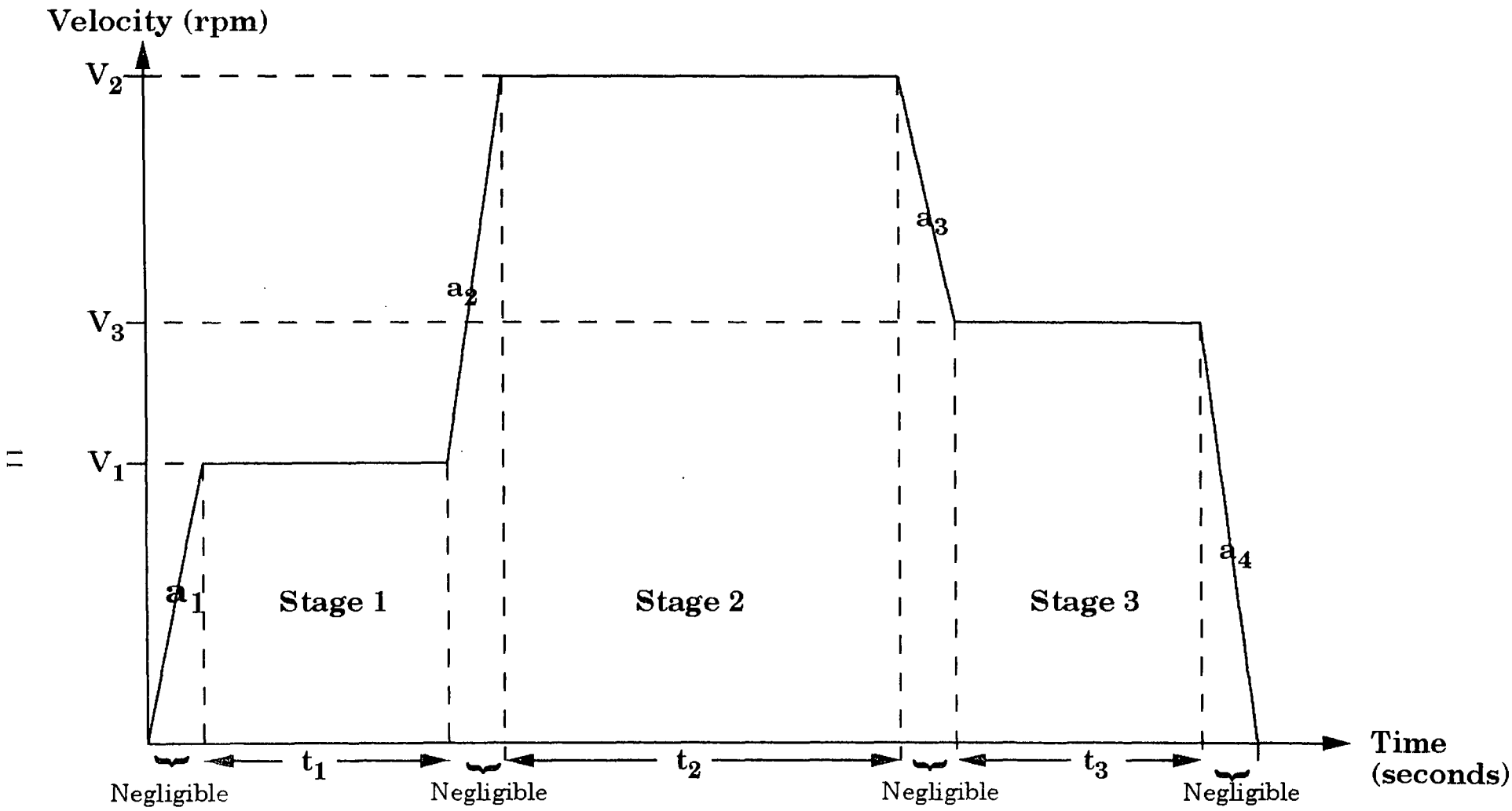

Figure 2.4. The three stages of the spinning process.

The infra-red lamp, which could be placed directly above the spinning substrate, was an optional extra. Figure 2.1 shows this set-up. The heater required calibrating. Therefore, a thermocouple attached to a silicon wafer was placed on the chuck support. Connected to it were two platinum wires which were linked to a digital temperature read-out. It was found that the infra-red lamp could be varied between 0°C and 350°C.

2.2 Preparation of the polyaniline solution

The priority was to work with a lump-free solution of polyaniline (see Figure 2.10). Otherwise, when spinning onto a substrate an uneven film was formed, resulting in undesirable and unreliable data as can be seen from some of the gas sensing results in Chapter 4.

Initially, work was carried out to find a suitable solvent in which to dissolve the polyaniline. It is thought that a polymer is most readily dissolved in a solvent which has a similar solubility parameter, δ (and this is defined as the mass of a solute required to saturate 100g of solvent at a given temperature). However, the solubility parameter, δ, of deprotonated emeraldine-base polyaniline (a blue/violet powder) is unknown. It is known that emeraldine base polyaniline is produced by oxidative polymerisation of aniline, whose δ value is reported to be 10.3 [2]. Therefore, it is reasonable to assume that the δ value for polyaniline has a similar value and that solvents with a δ value between 8 and 12 may be considered as suitable. As a consequence, a variety of solvents were mixed with polyaniline powder at various concentrations and inspected to see how well the solute dissolved. The results are shown in Table 2.1.

It is known that the bulk of easy solvents to work with are not strong enough to dissolve polyaniline. However, as can be seen from Table 2.1, some of the best solvents used to dissolve polyaniline are

N-methyl-2-pyrrolidone (NMP) and dimethyl sulfoxide (DMSO). NMP has a solubility parameter, δ, of 11.3 whereas for DMSO δ is 12. This implies that emeraldine base polyaniline must have a δ value in the region of 11-12.

Solvent tried:-	Results
N-methyl-2-pyrrolidone (NMP)	Mixed well, good solvent - blue/violet coloured solution.
NMP and chloroform	Poor solvent - blue solution.
NMP and hexane	Poor solvent - Oily, grey/black solution.
Dimethyl sulfoxide (DMSO)	Mixed well, good solvent - green solution.
NN-Dimethyl formamide	Poor solvent - blue solution.

Table 2.1. The solvents used to dissolve polyaniline .

It was decided that NMP should be used as the solvent [3] (although it has a high boiling point, 202°C and is therefore difficult to work with), since DMSO appeared to protonate the polymer. This was inferred from the fact that DMSO solution turned green, the characteristic colour of doped polyaniline. This is clearly undesirable if work is to be carried out on the deprotonated form.

Having decided which solvent to use, the next process was to try and deposit a solution onto a suitable substrate. Initial experiments involved making up a solution and spin-coating it onto the substrate (for our purposes here the solution was spun for a short length of time at a relatively slow speed). The percentage weight of polyaniline in solution was noted, as were the effects of spinning. It was found that for a solution

containing less than 1% weight of polyaniline, most of the polymeric material was thrown off the substrate during spinning (i.e. the solution was too dilute). Any that was left on the substrate dried very quickly as it was so thin, but subsequently turned green (i.e. the NMP evaporated off, leaving the thin polyaniline film, which was then doped in the surrounding atmosphere). However, for a solution with more than 12% weight of polyaniline present, the opposite occurred during spinning (i.e. the solution would not spread out on the substrate). Such a sample took well over twenty-four hours to dry, (in a fume cupboard) and for any excess NMP to evaporate off. The best solutions to spin though, had between 5% weight - 10% weight of polyaniline in solution and these took up to twenty-four hours to dry in a fume cupboard.

To spin on a glass substrate (coverslide) it was important to make sure that the substrate itself was properly cleaned. This involved the removal of any grease, dust particles etc., which could interfere with the quality of the spin-coated film [4]. Several preparative methods were tried out before deciding the best to use and these are listed below:

(a) Cleaning with acetone and isopropanol (IPA) solution, in a fume cupboard (thought to minimise dust particles).

(b) Washing with isopropanol and drying with nitrogen gas.

(c) Cleaning with tepol (a powerful detergent) and deionised water in an ultrasonic bath, in the clean room for thirty minutes and then refluxing with isopropanol for a further thirty minutes.

(d) Immersing in isopropanol for one hour in a clean room environment, then drying off with nitrogen gas.

(e) Immersing in isopropanol in an ultrasonic bath for one hour, in a clean room environment.

From the results of these experiments, it was decided that the best way to clean the glass coverslides was to immerse them in IPA (method

(d)). The length of time over which this was carried out was extended over 12 hours, typically. The use of a PTFE glass holder ensured that several slides could be cleaned at once without any of them coming into contact with each other. Following this, the coverslides were dried using compressed nitrogen gas. This procedure was also carried out in a fume cupboard in a clean room environment, which was relatively free of dust particles.

The actual glass substrates used were also of importance. Initially, standard glass microscope slides were used (with dimensions 3" by 1"). However, these were found to be too large for the spinner to cope with, as the vacuum holding the slide was not strong enough and so the slides were liable to spin off. A much more manageable substrate could be produced by cutting the microscope slides into eight rectangular pieces. A smaller substrate area also meant that the whole surface could be covered with the polyaniline solution. The only problem with these rectangular samples though, was with the unevenness of the spun solution around the edges. Therefore, circular coverslides were used and these afforded a distinct improvement in the surface quality.

When carrying out optical measurements (as discussed in Chapter 3), two types of substrates which had been spin-coated with polyaniline were used. Firstly, glass substrates were used to investigate any peaks at or above 300nm (as its lower wavelength limit is 300nm). Below this wavelength, sapphire substrates were used to see any ultraviolet peaks. The sapphire substrates were cleaned in exactly the same way as for the glass substrates.

Polyaniline was therefore dissolved in NMP and the solution processed to render it as homogeneous as possible. The main aim was then to remove as many lumps as possible, to give a solution of a high quality. This could be achieved in a combination of ways. Either:

(a) leaving the solution for an optimum length of time so as to ensure as many polymer chains as possible dissolved in the solvent;

Or,

(b) using mechanical methods to break down any remaining lumps (i.e either homogenising, centrifuging, ultrasonicating or filtering).

The centrifuge used was an Eppendorf Hermell Z320, capable of speeds up to 6000rpm. Unless specified, the solutions were spun at 4000rpm for thirty minutes. Under the force of gravity, the particles present were forced to sink to the bottom of the test tube. Once centrifuged, the lump-free solution could be decanted.

The homogeniser was an Ultra-Torrax instrument, capable of mixing at up to 25000rpm. It used a grinder, which spun at high speeds, to break up the particles in solution. Solutions were homogenised at 20500rpm for ten minutes, unless specified otherwise.

The ultrasonic bath vibrated the solution at a certain frequency, which, in theory, should also have the effect of breaking down the particles. Finally, filtering was also tried, to remove the lumps and the filter used possessed 0.5μm wide pores.

Solutions of different concentrations were made up by adding $(100 - x)\%$ of NMP solvent to $x\%$ of polyaniline (where x represents the percentage of polyaniline by weight, in solution). Initially, a 10% polyaniline solution in NMP was made up and spun onto a glass coverslip (which had been stringently cleaned). To get an idea of the quality of the film, a photograph of it was taken under a microscope, as can be seen in Figure 2.5 (the film is extremely lumpy). As an initial exercise this gave a very important result and from this starting point different solutions were made up, left for various lengths of time before being centrifuged etc., spun and then photographed (to monitor the film quality). This continued until the

$x\%$ (percentage of polymer in solution)	Length of time solution left	Preparation method	Comments
10	None	None	Very lumpy film See Figure 2.5
10	None	Ultrasound	Very lumpy film
10	None	Centrifuged	See Figure 2.6
10	None	Ultrasound and centrifuged.	No difference, film quality still very poor
10	None	Centrifuged and ultrasound	
10	None	Polyaniline added gradually	Polyaniline mixed into the solvent using a magnetic stirrer
10	None	Polyaniline added gradually and centrifuged	No change in spun films, still extremely lumpy
10	24 Hours	Centrifuged and ultrasonic bath	Smaller, more even lumps
10	24 Hours	Centrifuged	Distinct improvement, see Figure 2.7
10	24 Hours	Centrifuged 400rpm, Centrifuged 800rpm, Centrifuged 1200rpm	Controlled experiment. At higher speed we get a better film (less lumps, more even)
10	40 Hours	Solution gelled	Thought to be due to cross linking of the polymer chains

5	48 Hours	Centrifuged	Lots of small lumps on the film. See Figure 2.8
5	48 Hours	Centrifuged three times- each time using the solution decanted from the top region	Excellent film See Figure 2.9
5	48 Hours	Ultrasonic bath and centrifuged	Fewer, smaller lumps seen on film
5	48 Hours	Ultrasonic bath	Large, irregular lumps, not evenly spun
5	48 Hours	Homogenised	An excellent film-large lumps have been ground down. See Figure 2.10
5	48 Hours	Filtered	Excellent film
1	48 Hours	Filtered	Not as good as 5%-dopes easily as it is such a thin film
1	48 Hours	Filtered and centrifuged	Small frequent lumps on film

Table 2.2. The experimental techniques for solution preparation.

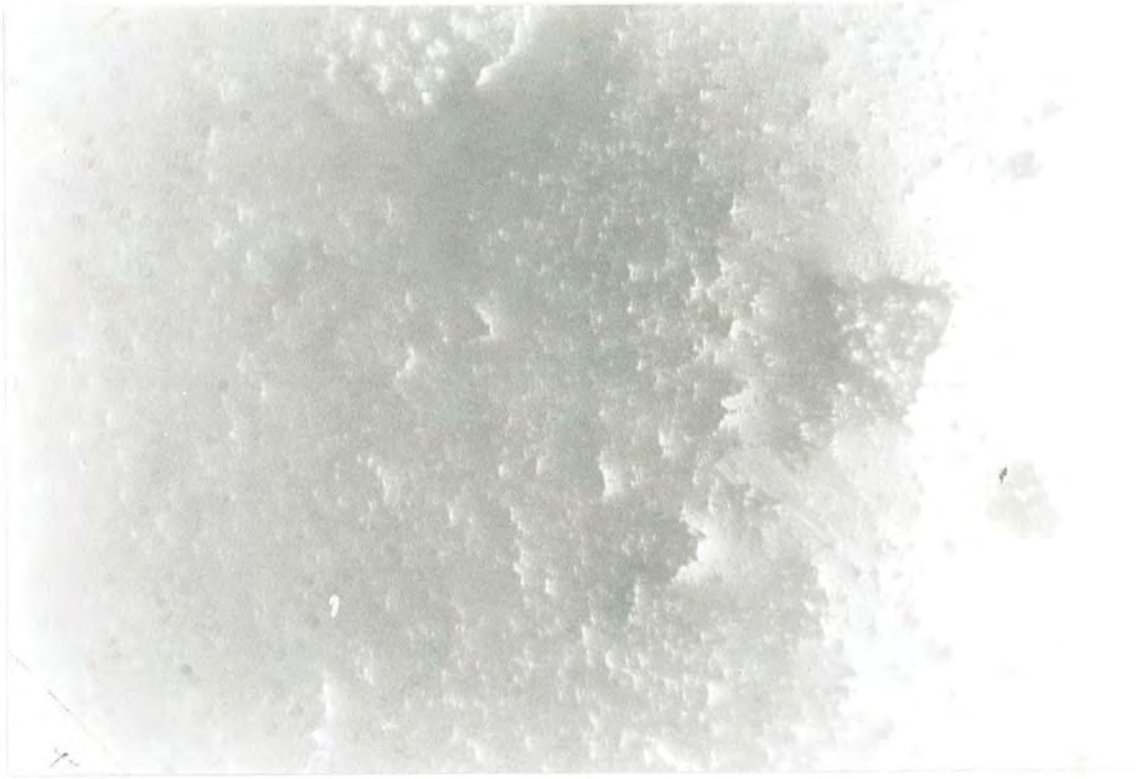

Figure 2.5 A 10% polyaniline solution just been made, then spun.

(Magnification x 4)

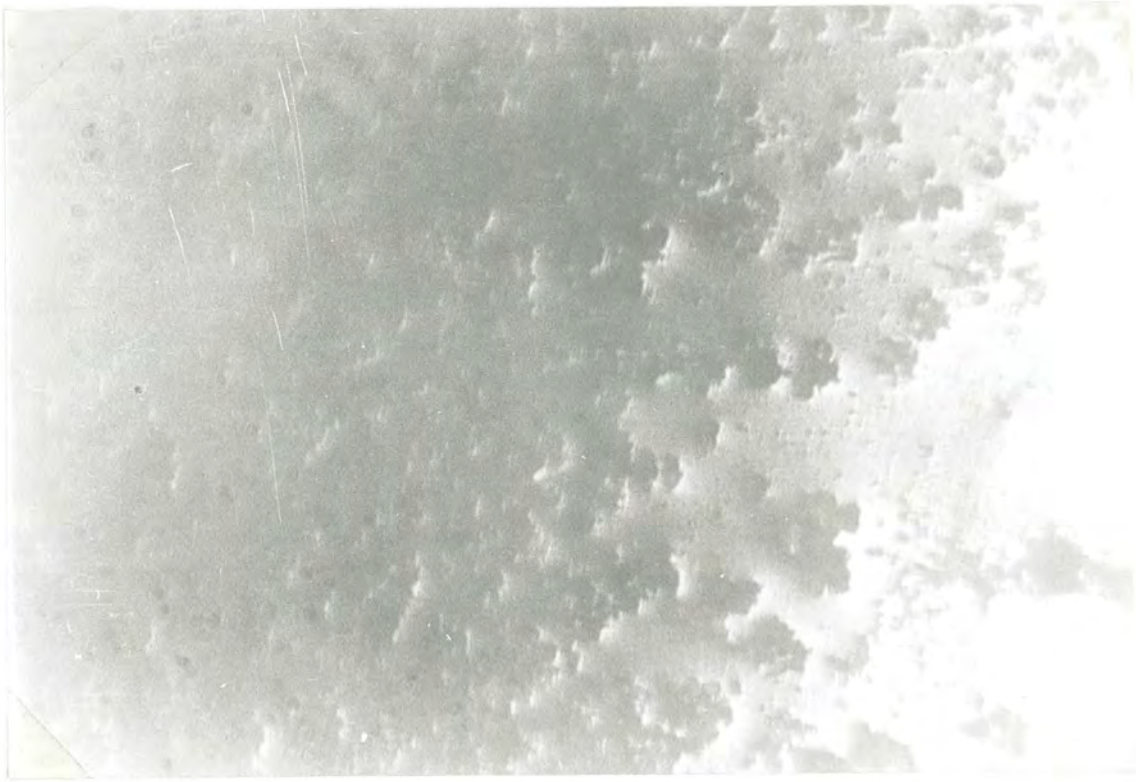

Figure 2.6. A 10% polyaniline solution, just made, centrifuged and spun.

(Magnification x 4)

Figure 2.7 A 10% polyaniline solution left for 24 hours, centrifuged then spun.

(Magnification x 4)

Figure 2.8. A 5% polyaniline solution, centrifuged and spun.

(Magnification x 4)

Figure 2.9 A 5% polyaniline solution left for 48 hours, centrifuged three times then spun.

(Magnification x 4)

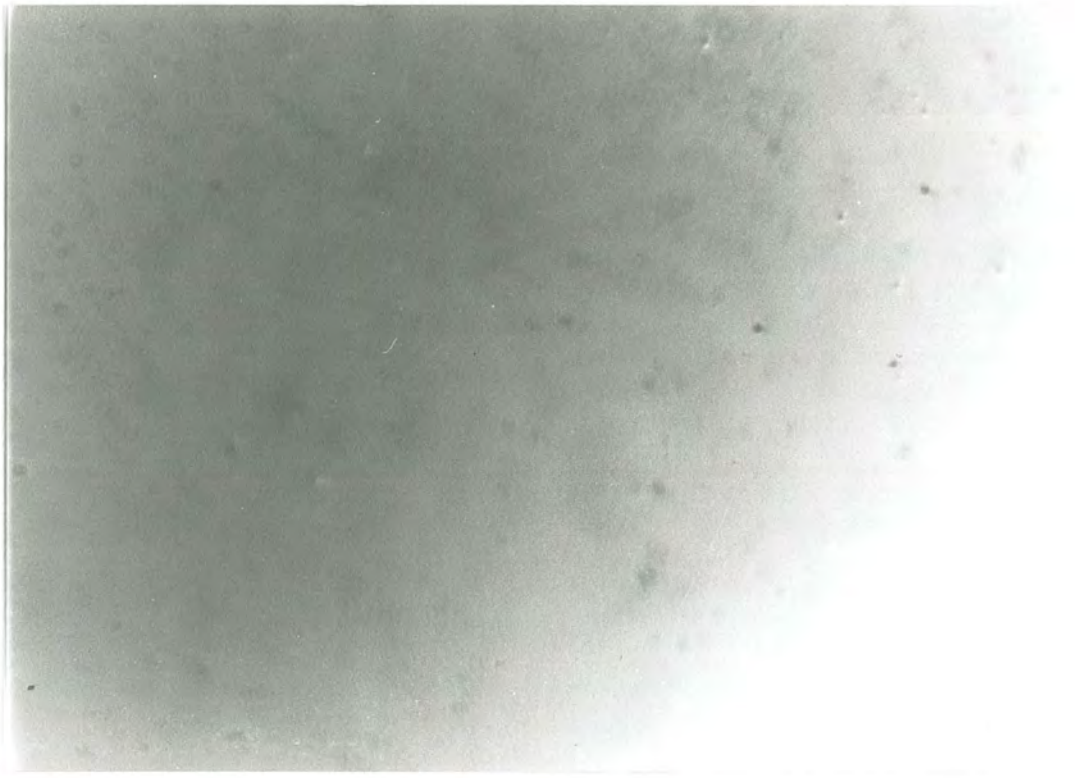

Figure 2.10. A 5% polyaniline solution, left 48 hours, homogenised and spun.

(Magnification x 4)

best, high quality film had been found. The experimental conditions tried and tested at room temperature are summarised in Table 2.2.

By comparing the six film surfaces in turn, (for polyaniline solutions processed in different ways) in Figures 2.5 - 2.10, an improvement is evident. The best solution to work with appears to be that containing 5% of the polymer which had been left to stand for forty-eight hours. Then, by either centrifuging this solution three times, or homogenising it before spinning, high quality lump-free films can be achieved. These are shown in Figures 2.9 and 2.10.

It was important to produce lump-free solutions with which to spin high quality films. Another important consideration was to spin level films, of a known thickness. It was necessary to investigate the effect of varying certain parameters on the final thickness of the spin-coated film. Therefore, work was carried out on solutions with different concentrations, solutions of the same concentration which had been left for different lengths of time before being spun, solutions of the same concentration which had been prepared by different mechanical methods and solutions which had been heated while they were being spun. The thickness of each film spun was then measured using a Tencor 100 Alpha-step. This instrument provided a thickness measurement across the film.

2.3 Results

(a) Thickness versus spin speed

All films were spun to a thickness in the order of micrometers. The results for the variation of thickness with spin speed (i.e. at stage two) are shown in Figure 2.11. It can be seen that for each solution, the final film thickness decreases with an increase in spin speed, a result which is to be expected. The 5% solutions decrease approximately exponentially, an effect

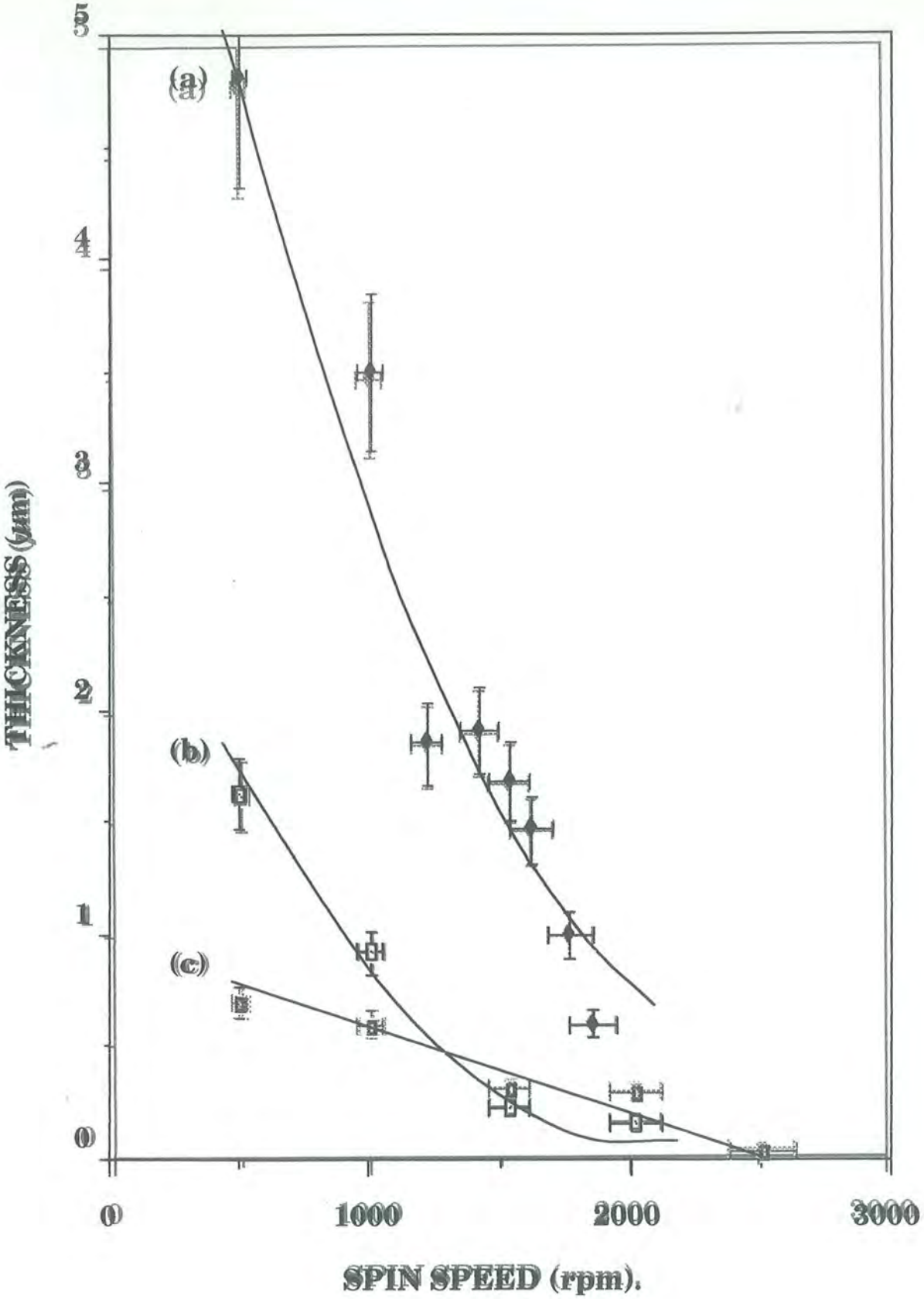

Figure 2.11. Thickness versus spin speed for (a) 5% solution left 48 hours, (b) 5% solution left 386 hours, (c) 1% solution left 96 hours.

which has been seen in many other polymers i.e. PMMA [1], whereas the 1% solution decreases linearly. At present, this difference is not fully understood.

Figure 2.11 shows that the length of time a solution is left standing before being spun, actually affects the final thickness. The solubility of polyaniline in the NMP solvent is an important consideration here. The polyaniline used was always of the same physical and chemical form and the solutions were made under the same conditions. It is known that solubility is determined by the internal pressure of the solvent [5]. Also, as noted by Van Krevelen [6], solubility decreases as the molecular weight of the solute increases (i.e. by increasing the amount of solute into a solution, it becomes harder it is for the solute to dissolve). These offer some explanation as to why the 5% solution left for 386 hours formed a thicker film than the 1% solution left for only 96 hours. On a microscopic scale, for a higher concentration solution, there will be more molecules present and if they have not been left for long enough in solution, they will not have had a chance to dissolve in the solvent. Therefore it is expected that the 5% solution left for 48 hours should form a thicker spin-coated film than the 5% solution left for 386 hours.

(b) Preparation of the solutions

Having found the best solutions to work with (i.e. 5% solution left for 48 hours, then either centrifuged three times or homogenised), the effect of spin speed on thickness has been investigated for three solutions which have been processed differently, Figure 2.12. The data for the different solutions are similar. However, it is worth noting here that the films spun at low speed show a lot of scatter amongst the experimental points. The spinner does not spin fast enough at low speeds to spin off any excess solution. Hence the film thickness may be more dependent on the initial

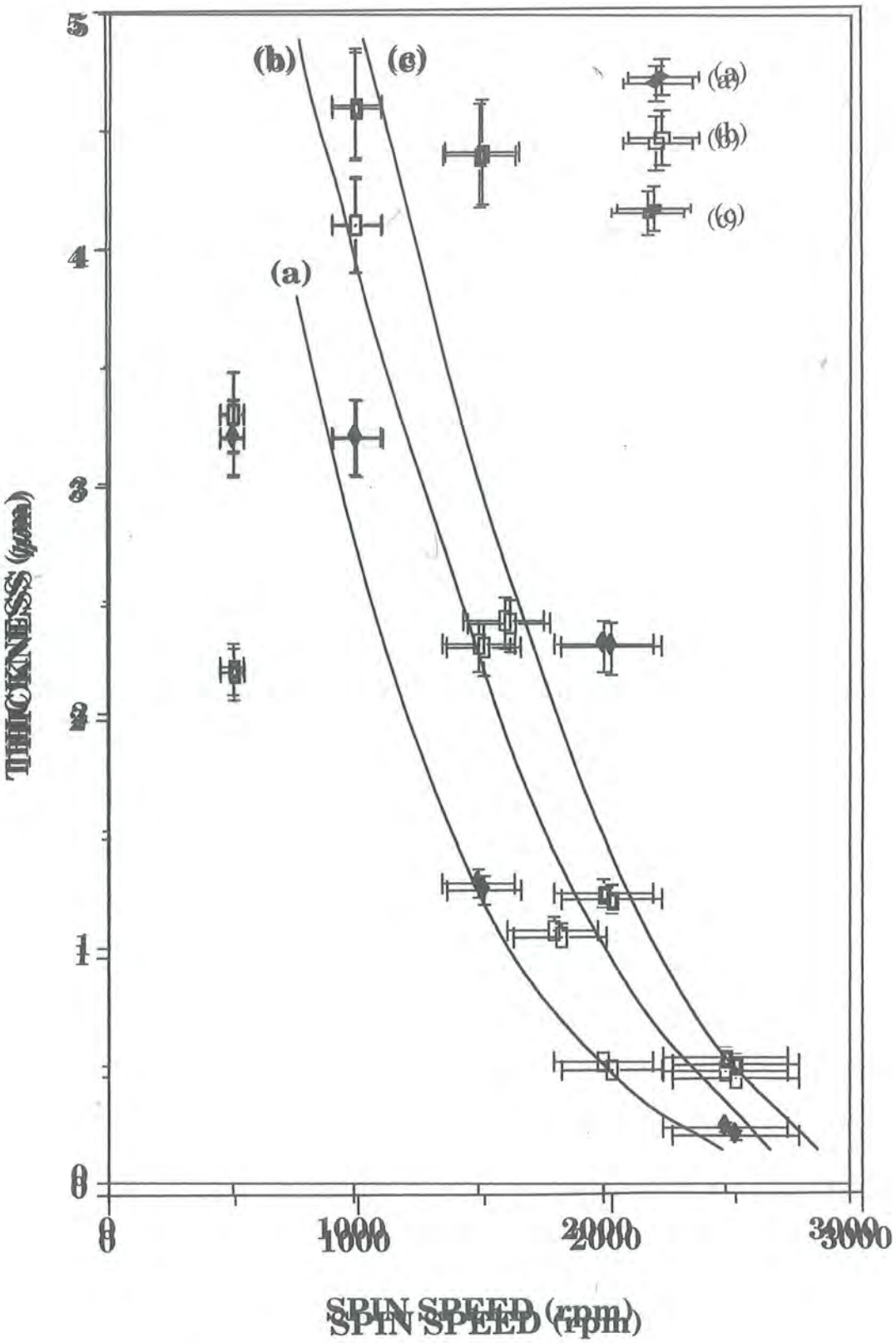

Figure 2.12. The variation in thickness with spin speed for films made from different solutions (a) 5% centrifuged 3 times (b) 5% homogenised (c) 5% homogenised and centrifuged.

Figure 2.12. The variation in thickness with spin speed for films made from different solutions (a) 5% centrifuged 3 times (b) 5% homogenised (c) 5% homogenised and centrifuged.

amount of solution put onto the substrate than the actual speed at which it had been spun.

(c) Thickness versus time

The variation of thickness with spinning time (see Table 2.3 for the relevant spinning conditions), as shown in Figure 2.13, is approximately exponential. This result can be compared to that of Daughton and Givens [1], who also find that thickness varies exponentially with spin speed.

Acceleration (units).	Velocity (rpm).	Time (seconds).
$a_1 = 10$	$v_1 = 570$	$t_1 = 60$
$a_2 = 100$	$v_2 = 1600$	t_2 = varied *
$a_3 = 10$	$v_3 = 230$	$t_3 = 60$
$a_4 = 10$		

* t_2 is varied from 20s-180s.

Table 2.3. The spinning conditions used to investigate the effect of varying spin time, on the outcome of the spun film.

(d) Thickness versus concentration

The variation of thickness with spin speed for different concentration solutions was investigated in more detail. The results are shown in Figure 2.14. The thickness is observed to decrease as spin speed increases, for all concentrations. Generally, the higher the concentration, the thicker the film, as also noted by Weill and Dechenaux [7]. This behaviour is dependent on the solubility of the polymer in the solvent, which in turn depends on how much polymer has been added to the solvent.

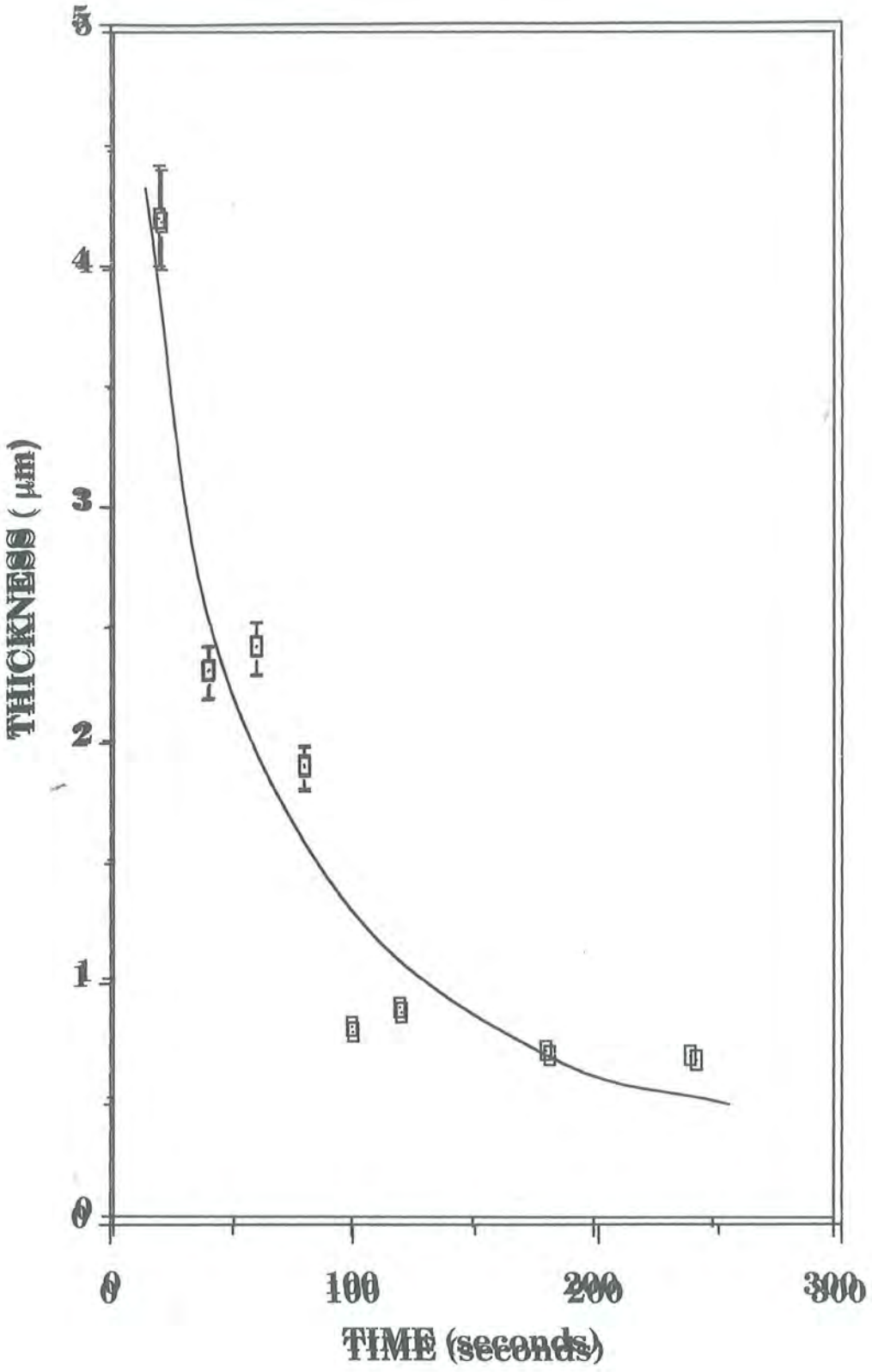

Figure 2.13. The variation of thickness with time for a 5% solution which had been left for 48 hours then homogenised and spun at 1600rpm (i.e $v_2 \equiv$ 1600rpm).

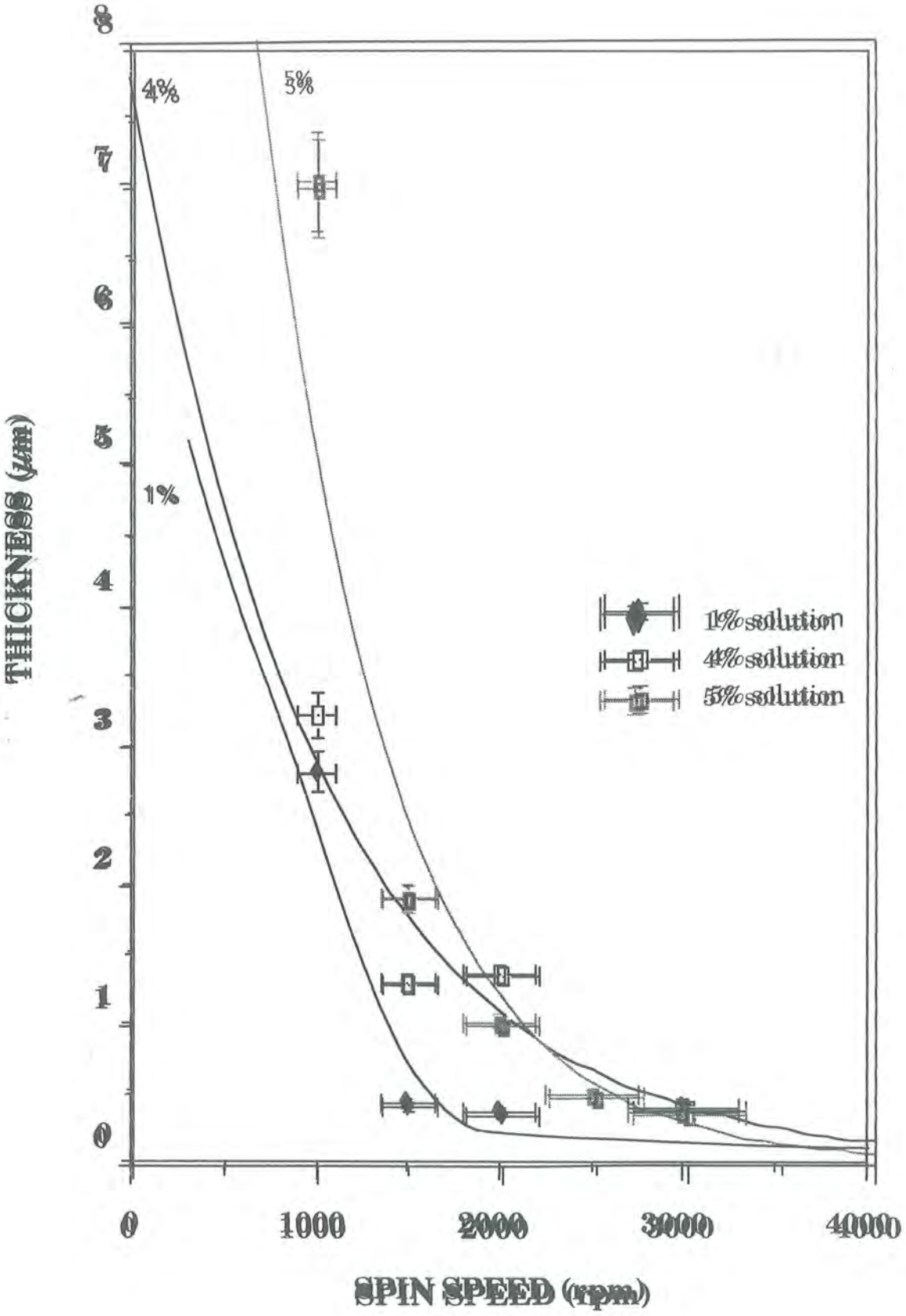

Figure 2.14. The variation in thickness with spin speed for three solutions of different concentration.

Figure 2.14. The variation in thickness with spin speed for three solutions of different concentration.

A guide to the eye only ... Please lift

It is also interesting to note the behaviour of the 1% solution. This shows an exponential dependence in Figure 2.14, but a similar plot in Figure 2.11 shows linear characteristics. The difference is due to the factthat one solution has been made up and left for 96 hours (Figure 2.11) where as the other has only been left for only 48 hours. Therefore, the length of time a solution is left before being spun, does seem to have an effect on the film thickness.

Figure 2.15 shows the variation of thickness with concentration for solutions spun at 1500rpm and 2000rpm, respectively. As can be seen, both curves are similar, but the solutions spun at 2000rpm form thinner films.

(e) The effect of heating

The infra-red lamp was placed over the spinning substrate from the start of stage two and remained in place until the process was completed.

Up to 80°C, the film remained wet (i.e, the lamp had little or no visible effect). At 100°C, the films spun were uneven. A thick band of solution was left around the edge of the substrate, while in the centre, a circular patch had dried. This was because during the spinning stage, when any excess solution was spun off (or at least spun to the edge of the substrate), the central region was thin enough for the excess residues and solvent to evaporate off. However, the outer band of solution was too thick for there to be a noticeable amount of drying.

By heating up to 120°C, an excellent homogeneous film could be spun. During the spinning stage, most of the solvent evaporated. Therefore, during the deceleration stage, a much thinner band formed around the edge (although still not completely eliminated).

Heating up to 175°C did not improve the quality of the spun film. However, there was a change in colour, from light blue to a dark metallic purple/blue. This was due to thermal crosslinking of the polymer chains [8]

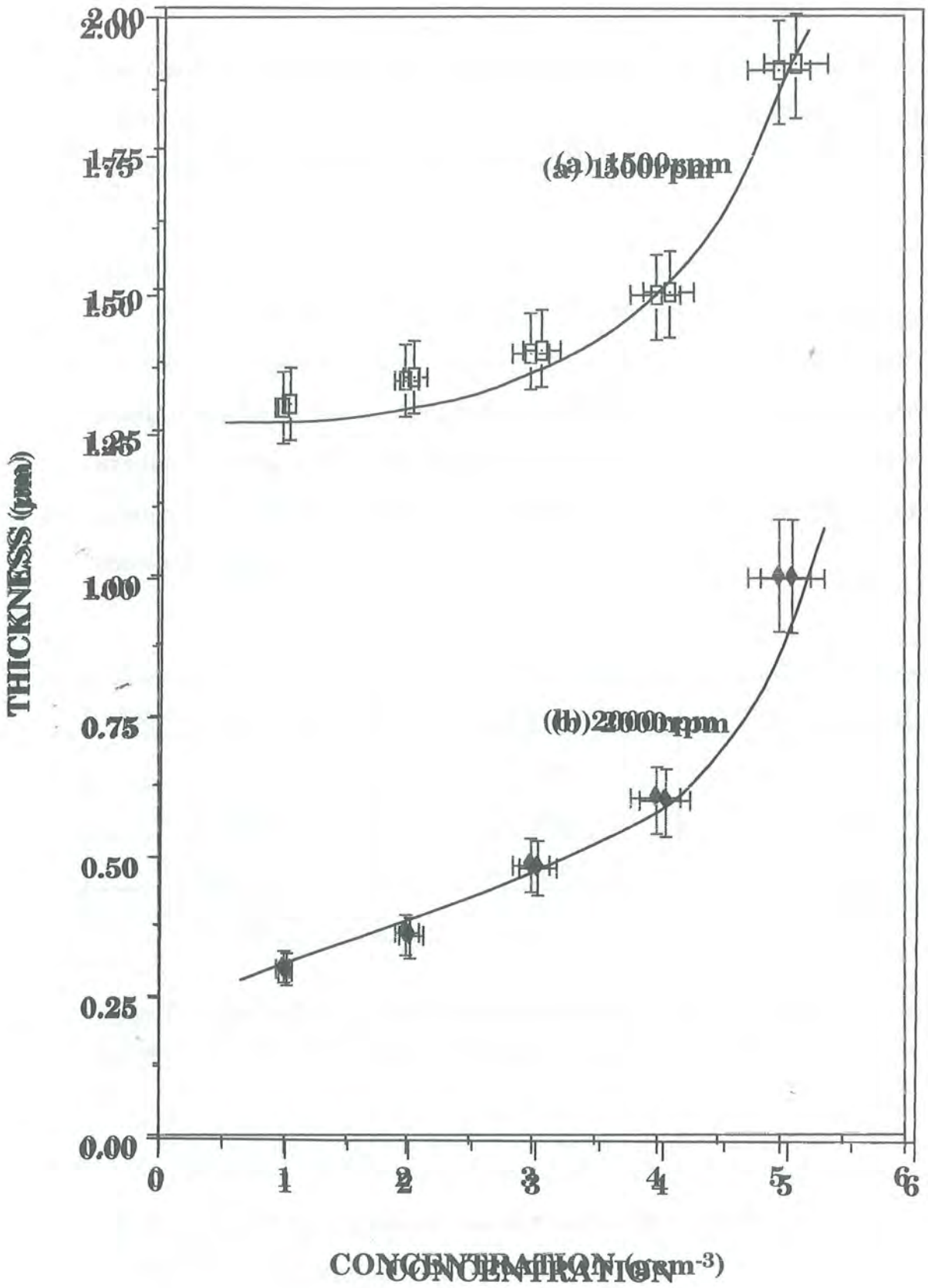

Figure 2.15. A comparison of thickness with concentration for polyaniline films spun at (a) 1500rpm and (b) 2000rpm.

Figure 2.15. A comparison of thickness with concentration for polyaniline films spun at (a) 1500rpm and (b) 2000rpm.

and also to the oxidation of the spin-coated film. As our aim was to produce high quality films of deprotonated emeraldine-base polyaniline, any change in the chemical structure of the film was undesirable.

(f) Levelling the spin-coated film

Controlled experiments were carried out on the spinner parameters, to find which could further improve the quality of a spun film, fabricated using a heater to 120°C. (Such films still had a thick ring of polyaniline around the edge of the substrate and it was found that this could not be removed by heating alone). The starting point was using the conditions shown in Table 2.4.

Acceleration (units).	Velocity (rpm).	Time (seconds).
$a_1 = 10$	$v_1 = 570$	$t_1 = 60$
$a_2 = 100$	$v_2 = 1800$	$t_2 = 60$
$a_3 = 10$	$v_3 = 390$	$t_3 = 60$
$a_4 = 10$		

Table 2.4. The spinning conditions used when trying to remove the ring of polyaniline around the edge of the substrate of a spun film.

From here the following parameters were changed, one at a time and the spun films were examined visually to find the best film.

(a) decreased deceleration time, $t_3 = 10$s.

(b) decreased deceleration speed, $v_3 = 230$rpm.

(c) both (a) and (b), $v_3 = 230$rpm and $t_3 = 10$s.

(d) increased deceleration time, $t_3 = 40$s.

(e) increased deceleration speed, $v_3 = 720$rpm.

(f) both (d) and (e), $t_3 = 40$ and $v_3 = 720$rpm.

(g) increase deceleration time, decrease deceleration speed, $t_3 = 40$s and $v_3 = 230$rpm.

(h) decrease deceleration time, increase deceleration speed, $t_3 = 10$s and $v_3 = 720$rpm.

(i) as for (c) and also increase final ramp, $a_3 = 20$, $v_3 = 230$rpm, $t_3 = 10$s.

(j) as for (c) and also decrease final ramp, $a_3 = 5$, $v_3 = 230$rpm, $t_3 = 10$s.

(k) as for (f) and increase final ramp $a_3 = 20$, $t_3 = 40$s, $v_3 = 720$rpm.

(l) as for (f) and decrease final ramp, $a_3 = 5$, $t_3 = 40$s, $v_3 = 720$rpm.

It was found that by decreasing the deceleration speed by up to one half of the original value, the film spun was of a much higher quality. The thick ring of polyaniline around the edge was no longer a prominent feature, although not totally removed. A slower deceleration speed, i.e., $v_3 = 230$rpm, ensured that the solution around the edge was not dispersed across the substrate, upsetting the level film formed. The spinning conditions which gave the best film are summarised in Table 2.5.

It is interesting to speculate on the reason for this improvement in film quality. It was realised that the spin-coating of polymer films is a complex process [9] and a number of possible mechanisms must be considered.

To try to explain what is happening during the spinning process, the polyaniline solution may be considered in terms of a Newtonian and a non-Newtonian fluid. The term 'Newtonian' implies that the viscous behaviour of a model fluid can be represented by a simple relation i.e. shear stress, τ, is proportional to velocity gradient, (otherwise known as Force/Area). This is represented diagrammatically in Figure 2.16. The relationship closely

approximates the behaviour of many real fluids, [10] and can be represented graphically in Figure 2.17.

Acceleration (units).	Velocity (rpm).	Time (seconds).
$a_1 = 10$	$v_1 = 570$	$t_1 = 60$
$a_2 = 100$	$v_2 = 1800$	$t_2 = 60$
$a_3 = 10$	$v_3 = 230$	$t_3 = 60$
$a_4 = 10$		

Table 2.5. The spinning conditions which produced the most evenly spun film of polyaniline.

A non-Newtonian fluid is one in which the viscosity, μ, is not constant at a given temperature and pressure but is dependent on the rate of shear, ψ in the fluid and the apparatus in which the fluid is contained. Non-Newtonian fluids can be defined in the following terms [11]:

(i) The shear at any point is a function of shearing stress (τ) only.

(ii) The relationship of shear stress, τ, with rate of shear, ψ, depends on the time for which a fluid has been sheared.

(iii) One which has characteristics of solids or fluids and exhibits partial recovery after deformation (i.e. starts off as a Newtonian fluid but ends up behaving as a non-Newtonian fluid).

It is not possible from the work carried out here on the polyaniline solution to state conclusively whether it behaves as a Newtonian or a non-Newtonian fluid. It could be assumed to be either due to its behaviour while being spun. For example, Newtonian fluid behaviour is indicated by forming a level film (of constant thickness), as can be seen from Figure 2.17, while a non-Newtonian fluid does not.

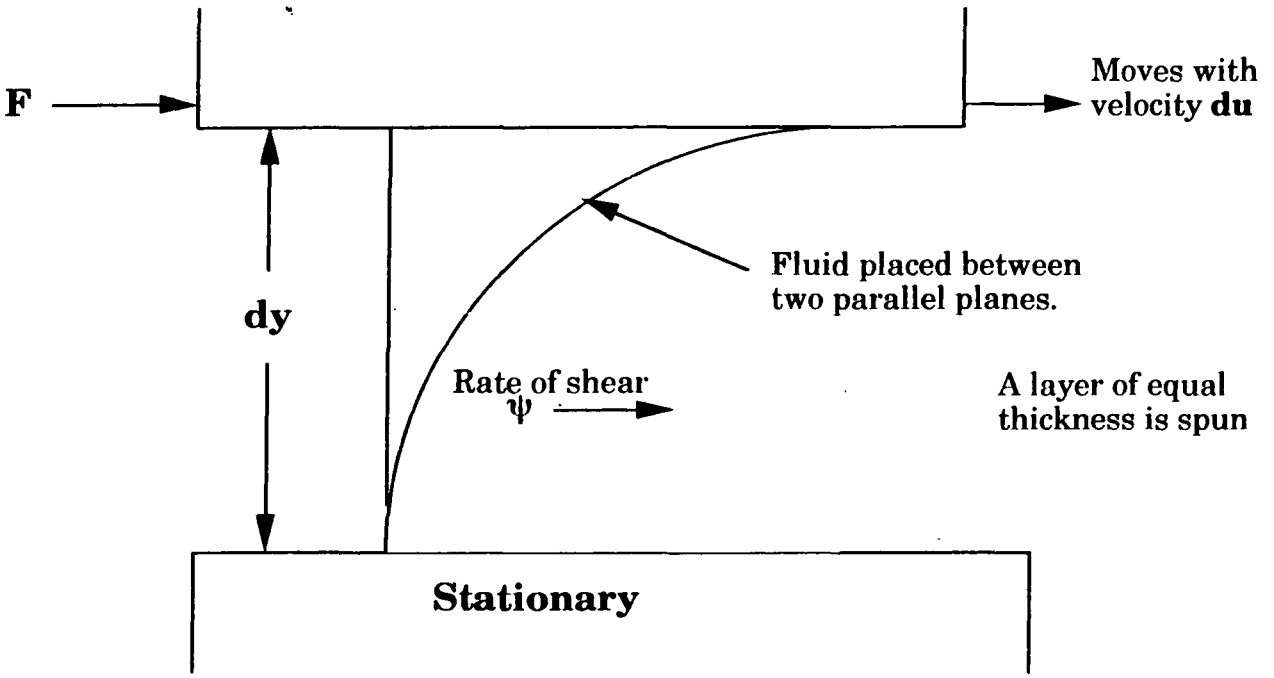

μ = viscosity (tangential force per unit area exerted on layer of fluid, a unit distance apart). For a Newtonian fluid, shear stress is proportional to velocity gradient, i.e. F/A.

Figure 2.16. A Newtonian Fluid.

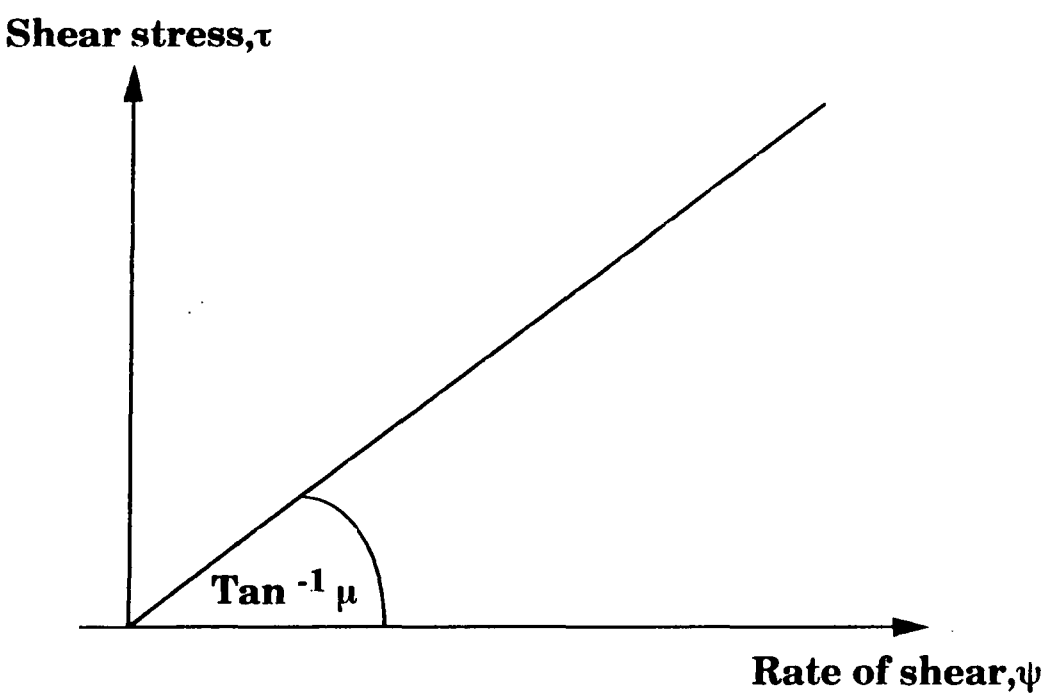

Figure 2.17. The relationship between viscosity μ, shear stress τ and rate of shear ψ, for a Newtonian fluid. A film of equal thickness is formed.

Although a level film of polyaniline was spun, it is not known exactly what happens to the solution during each stage of the process and so it cannot be assumed to be a Newtonian or a non-Newtonian fluid. Research which has been carried out on other similar fluids may give some ideas as to why polyaniline behaves as it does. Several theories which have been put forward are discussed briefly below:

A model proposed by Jenekhe and Schuldt, the Carreau Model [12] states that for a non-Newtonian fluid during the spin-coating process, it behaves more like a Newtonian fluid as it gets thinner. In general, however, it has been found that for spinning at faster spin speeds (i.e.greater than 1000rpm), films of greater uniformity will be produced [9]. This has also been found by Givens and Daughton [7] who state that non-uniformity in spun films is connected to instabilities in the initial flow of the solution. These latter authors have also noted that using a very fast final spin speed (v_3) will give the most uniform film. However, this contradicts the results presented here.

Evaporation of the solvent during spinning has been investigated by Meyerhofer [13] and Sukanek [14]. Sukanek has noted that if a film is of uniform thickness, non-Newtonian effects cannot be the cause for the spin-speed dependence of thickness. Differences in this dependence are therefore probably due to evaporation effects. Following on from this, the spin-speed dependence has been suggested to be 'thickness is proportional to (spin speed)$^{1/2}$' for a Newtonian fluid which then undergoes evaporation [15]. Applying this theory to the results in Figure 2.11, it can be seen that they only agree at low spin-speeds. However, it is known that more even films are spun at higher spin-speeds. As the boiling point for NMP is 202°C and all of the films spun were not dry immediately (taking up to 24 hours by slow evaporation, unless the infra-red lamp was used), it is unclear as to whether Sukanek's theory can be applied to polyaniline spun-films.

Perhaps the most applicable model is that by Lawerence [9], which incorporates both Newtonian and non-Newtonian effects during the spinning process. It states that during the first stage of spinning, the fluid is thought to behave like a non-Newtonian fluid. During the second stage of spinning, the inertial and non-Newtonian effects become negligible and the initial conditions have been forgotten. The fluid from then onwards is assumed to behave in a Newtonian manner. However, this area of research on polyaniline is open to further study.

2.4 Conclusions.

To spin a high quality film of deprotonated emeraldine-base polyaniline onto a glass substrate, two areas have been investigated: quality control of the polyaniline solution and processibility of the spin-coated films.

The quality control process involved the successful preparation of a lump-free solution. This depended on the concentration used, the length of time the solution was left and the preparation of the solution before it was spun. The optimum solutions to use were found to be of a 5% concentration, which had been left for 48 hours. Then the solutions were either homogenised at 20500rpm for ten minutes, or centrifuged three times at 4000rpm for thirty minutes.

Daughton and Givens [4] established that process variables strongly influence the final film thickness. For polyaniline, these variables include spin time, spin speed and concentration of the solution. It was found that the higher spin speeds (i.e., greater than 1000rpm) gave more even films.

It should be noted that the amount of solution dispensed onto the substrate did not affect the thickness of the film if it was spun at high speed (i.e greater than 1000rpm). Also, the quality of the film spun was not affected greatly by evaporation.

The behaviour of polyaniline as a Newtonian or non-Newtonian fluid has been considered. By comparing the experimental results on polyaniline with the research carried out on some other materials, polyaniline may be considered more favourably as a non-Newtonian fluid. Further study [16] has indicated that the solution can physically cross-link, not only by the way it is prepared, but also by exerting too much shear on it when it is being spun. At a high enough shear, a thick viscous fluid is formed and there is a critical shear point at which the fluid deviates from behaving in a Newtonian way. This would explain the form of the graphs plotted for 'Thickness Vs Spinspeed' (Figures 2.11 - 2.14).

References.

[1] A.Weill and E.Dechenaux - Polymer Engineering and Science, **28,** (1988), 945-948.

[2] Rubber Handbook - The Chemical Rubber Company, London.

[3] European Patent Application, No. 89117826.1.

[4] L.Holland - The properties of glass surfaces, Chapman and Hall, London, (1964).

[5] J.H Hildebrand and R.L Scott - The solubility of non-electrolytes, Reinhold Publishing, New York, (1949).

[6] L.Van Krevelen - Properties of polymers, Elsevier, Amsterdam, (1976).

[7] W.J Daughton and F.L Givens - The Journal of Electrochemical Society, **129**, (1982), 173 - 179.

[8] A.J Milton - Synthetic Metals, 1992. To be published.

[9] C.J Lawerence - Physics of Fluids, **31**, (1988), 2786 - 2795.

[10] S.J Peerless - Basic Fluid Mechanics, Pergamon Press, (1967).

[11] W.Wilkinson - Non-Newtonian Fluids, Pergamon Press, (1960).

[12] S.A Jenekhe and S.B Schuld - Industrial Engineering and Chemical fund, **23**, (1984) 432 - 438.

[13] D.Meyerhofer - Journal of Applied Physics, **49**, (1978) 3993 - 3997.

[14] P.Sukanek - Journal of Electrochemical Society, **138**, (1991), 1712 - 1719.

[15] T.O'Hara, Y.Matsumoto, H.Ohashi - Physics of Fluids **A1**, (1989), 1949.

[16] A. Monkman - Private Communication, Universityof Durham 1994.

Chapter 3

Optical studies of polyaniline thin films

3.0 Introduction

In this chapter, the optical properties of polyaniline are investigated experimentally. Information has been gathered about the structure of polyaniline and this is compared and contrasted to theoretical predictions [1].

3.1 Optical absorption in thin films

By measuring the optical absorption coefficient and sample thickness of a spun film, values of the refractive index, extinction coefficient and permittivity may be calculated for polyaniline.

The optical absorption coefficient has been defined clearly by Moss [2]. He states a simple relationship between the energy of an electromagnetic wave and distance. Basically, an electromagnetic wave will decrease in energy by the fraction e:1, over a distance $1/\alpha$ (where α is the absorption coefficient in a medium),

$$\frac{dI}{I} = -\alpha\, dx \qquad \ldots 3.0$$

A material of known thickness, x, has been deposited by the spin-coat technique. Electromagnetic waves of known intensity, I_0, are passed through the material [3] and the fraction of energy lost during the transmission through distance dx is given by

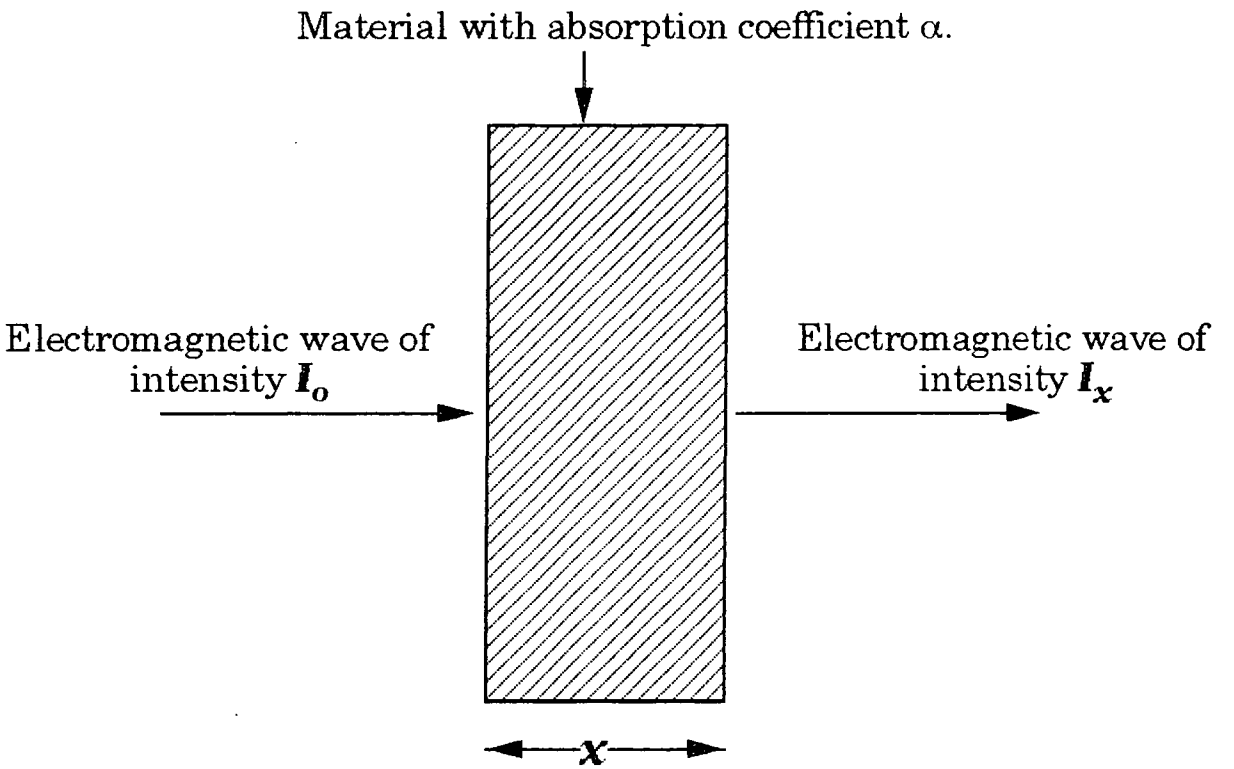

$$I_x = I_o \exp^{(-\alpha x)}$$

Figure 3.1. The Beer-Lambert Law.

$$\frac{1}{I}\, dI = -\alpha\, dx \qquad \ldots 3.1$$

where α is the absorption coefficient of the material (cm^{-1}). This relationship is known as the Beer-Lambert Law and is shown in simplistic terms in Figure 3.1. Integrating equation 3.1 we get

$$\int_{I_o}^{I_x} \frac{1}{I} dI = -\alpha \int_{0}^{x} dx \qquad \ldots 3.2$$

Therefore,

$$\ln I_x - \ln I_o = -\alpha x \qquad \ldots 3.3$$

So,

$$I_x = I_o \exp(-\alpha x) \qquad \ldots 3.4$$

It can be seen that there is an exponential decrease in the intensity of the electromagnetic wave on passing through the sample.

The attenuation of the wave across a thin sample can be studied in more detail [4]. The electromagnetic wave may be considered in terms of its magnetic and electric field components, using Maxwell's equations. As this is an absorbing media, it can be characterised by a complex dielectric constant, ε,

where

$$\varepsilon = \varepsilon_1 - \iota\varepsilon_2 = (n - ik)^2 \qquad \ldots 3.5$$

n = refractive Index

k = Imaginary part of refractive index

and

$$\alpha = \frac{4\pi k}{\lambda} \qquad \ldots 3.6$$

and λ is the wavelength in vacuo

The polyaniline spun sample is assumed to be of the form shown in Figure 3.2. The intensity of the wave can be described in terms of the amplitude of reflectance (R), transmittance (T). Initially, part of the wave amplitude is transmitted (t_1) and part is reflected (r_1). The transmitted component, t_1 is then again partly transmitted, (t_2) and partly reflected ($t_1 r_2$), and so on. Chopra [5} summarises the amplitude reflectance and transmittance such that:-

$$R_{amp} = \frac{r_1 + r_2 \exp(-2i\delta_1)}{1 + r_1 r_2 \exp(-2i\delta_1)} \qquad \ldots 3.7$$

where $\delta_1 = \frac{2\pi}{\lambda} . n_1 t \cos \varphi_1$ = Phase thickness of the film. ...3.8

$$T_{amp} = \frac{t_1 t_2 \exp(-i\delta_1)}{1 + r_1 r_2 \exp(-2i\delta_1)} \qquad \ldots 3.9$$

and r_1, r_2, t_1 and t_2 are the Fresnel Coefficients at the n_0/n_1 and n_1/n_2 interfaces.

The reflectivity and transmissivity (intensities) are given by:-

$$R = \frac{r_1^2 + r_2^2 + 2 r_1 r_2 \cos 2\delta_1}{1 + r_1^2 r_2^2 + 2 r_1 r_2 \cos 2\delta_1} \qquad \ldots 3.10$$

$$T = \frac{n_o}{n_2} . \frac{t_1^2 t_2^2}{1 + 2 r_1 r_2 \cos 2\delta_1 + r_1^2 r_2^2} \qquad \ldots 3.11$$

The expressions in equations 3.10 and 3.11 can be written in terms of their corresponding refractive indices and for normal incidence and transparent media (i.e. real n) they can be written as follows:-

$$R = \frac{(n_0^2 + n_1^2)(n_1^2 + n_2^2) - 4n_0 n_1^2 n_2 + (n_0^2 - n_1^2)(n_1^2 - n_2^2)\cos 2\delta_1}{(n_0^2 + n_1^2)(n_1^2 + n_2^2) + 4n_0 n_1^2 n_2 + (n_0^2 - n_1^2)(n_1^2 - n_2^2)\cos 2\delta_1} \quad \ldots 3.12$$

$$T = \frac{8 n_0 n_1^2 n_2}{(n_0^2 + n_1^2)(n_1^2 + n_2^2) + 4n_0 n_1^2 n_2 + (n_0^2 - n_1^2)(n_1^2 - n_2^2)\cos 2\delta_1} \quad \ldots 3.13$$

Chopra [5] quotes the transmittance of a film of refractive index $n_1 - ik_1$, by comparing equations 3.10 and 3.11 such that,

$$T = \frac{16 n_0 (n_1^2 + k_1^2)^2 \exp(-4\pi k_1 t/\lambda)}{[(n_1 + 1)^2 + k_1^2][(n_0 + n_1)^2 + k_1^2]} \quad \text{for } n_1 > n_0 \quad \ldots 3.14$$

Neglecting interference and multiple reflections, T and R are related by

$$T = (1 - R)^2 \exp\frac{(-4\pi k_1 t)}{\lambda} \quad \ldots 3.15$$

and if the reflection at the film/substrate interface ($n_0 < n_1$, $k_0 = 0$) is considered,

$$T = (1-R)^2 \exp\frac{(-4\pi k_1 t)}{\lambda} = (1-R)^2 \exp(-\alpha t) \quad \ldots 3.16$$

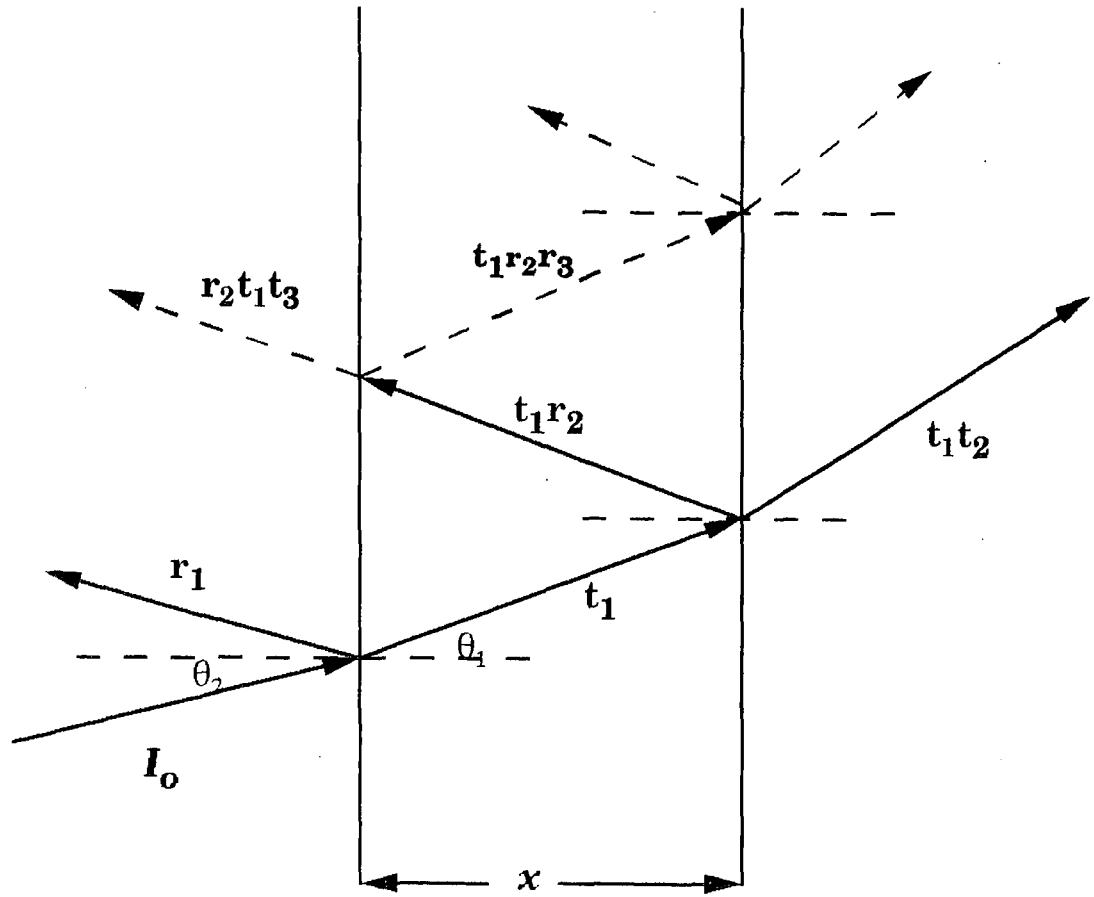

Figure 3.2. Reflection and transmission in an absorbing medium.

Rearranging equation 3.16 will give a value for the absorption coefficient at a particular frequency. Using this relationship, the absorption coefficient for polyaniline can be measured. Further to this work, the optical band gap of deprotonated emeraldine-base polyaniline can be accurately ascertained and compared to theoretical models.

3.2 Experimental method

Glass coverslips or sapphire substrates were cleaned in the usual manner (i.e left in an ultrasonic bath in acetone for one hour, then drying with a nitrogen gas gun). Meanwhile, a 5% solution of polyaniline in NMP which had been left for forty-eight hours was prepared by either;

(a) centrifuging for thirty minutes, at 4000rpm and repeated twice more;

or

(b) homogenising for ten minutes, at high speed up to 20500rpm, using the Janke and Kunkel Ultra-Turrax homogeniser.

The spinning conditions were altered slightly to those given in Chapter 2 and are shown in Table 3.1. After the first sixty seconds, the infra-red lamp was switched on at 100°C and left in place for the remaining two minutes. Heating the spun sample removed any NMP residue (although the boiling point of pure NMP solvent is 202°C, at atmospheric pressure) [6]. This was possible because the film being spun was a relatively thin film. Several different films were spun in order to investigate the effect of spin speed and hence film thickness on the optical absorption coefficient of polyaniline.

Optical measurements were carried out using a Perkin Elmer Lambda 19 spectrophotometer, which is a double beam instrument. The

samples of polyaniline under investigation behaved as absorbing materials The layout of the spectrophotometer is show in Figure 3.3.

The wavelength range was between 200nm and 3000nm. Between 3000-2000nm, absorbance due to water molecules can be seen [7]. As the lower wavelength limit of glass is approximately 300nm, to scan lower than this, a sapphire substrate must be used.

Acceleration (in units)	Velocity (rpm)	Time (seconds)
$a_1 = 10$	$v_1 = 3000$	$t_1 = 60$
$a_2 = 100$	v_2 = (varied)	$t_2 = 60$
$a_3 = 10$	$v_3 = 2200$	$t_3 = 60$
$a_4 = 10$		

Table 3.1 The spinning conditions used to prepare thin films of polyaniline for optical investigations, where v_2 was varied between 1500 - 3500rpm.

All scans were carried out at a speed of 960nm/minute and these were collected at intervals of 0.80nm. The smoothing factor (used to suppress excessive noise), was set to 0.1. If too high a value was used, this could lead to undesirable flattening of the scan and hence a distorted picture is obtained [8]. The slit width (which gives the spectral band pass or resolution) was set at 4.85nm.

(a) Transmission measurements

An initial calibration was carried out, so that the effect of the substrate (glass or sapphire) could be compensated for when doing the final calculations. Two cleaned substrates were placed in the sample cell and

reference cell (as can be seen in Figure 3.4) and a baseline scan was carried out.

By removing the uncoated substrate from the sample cell holder and replacing it with a spin-coated substrate, a scan showing the variation of transmission with wavelength could be plotted.

(b) Reflection measurements

After removing both of the sample holders from the sample compartment, a background calibration in air was carried out. A reflectance rig was positioned in the place where the sample holder had been and a special optical mirror was put on it. A scan was then carried out as a function of transmission. This formed the baseline for all the subsequent measurements.

Finally, the mirror was replaced by the spin-coated sample which had been mounted so that it faced downwards on the rig. Care was taken to ensure that the beam was directed at the sample and also that the same spectral region was scanned in both reflection and transmission experiments.

Once all of these measurements had been carried out, a profile of thickness across the region scanned by the beam was taken, using a Tencor 100 Alpha step. This was performed last as it was a destructive process.

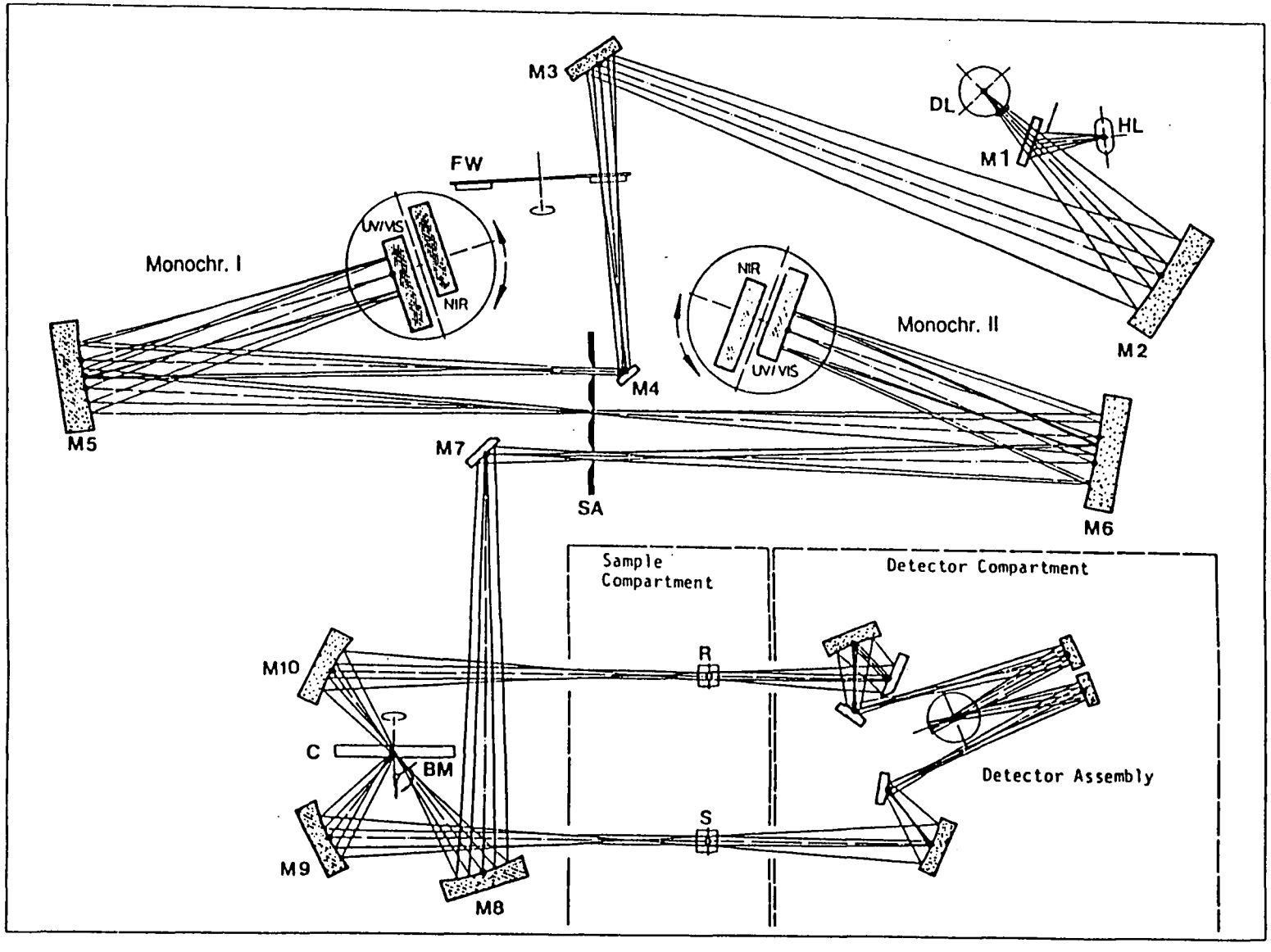

Figure 3.3. The layout of the spectrophotometer.

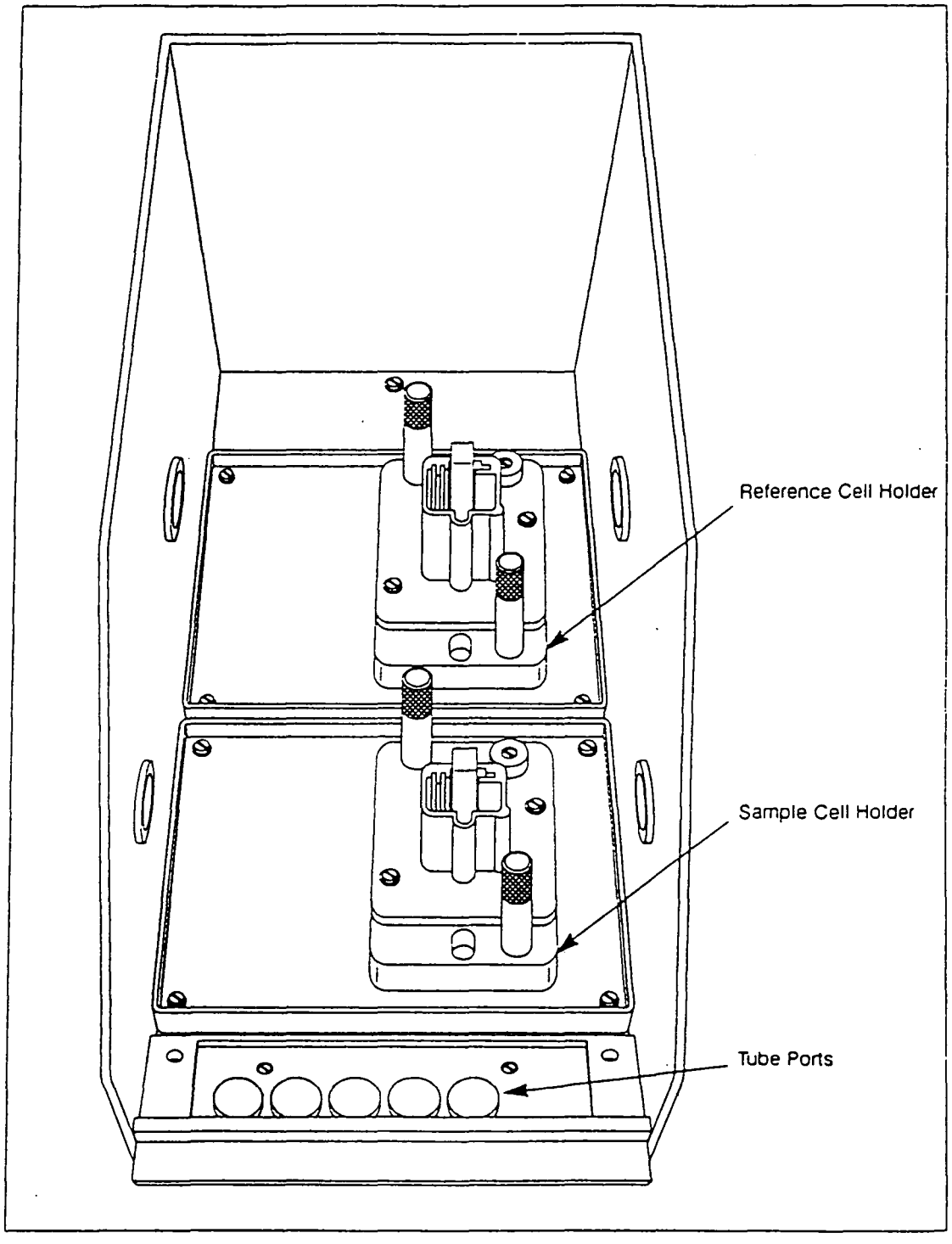

Figure 3.4. The sample and reference chambers of the spectrophotometer.

3.3 Results

Initially, transmission and reflectance were plotted as a function of wavelength. Figures 3.5 and 3.6 show these results, respectively, for a film 0.12μm thick, having been prepared from a homogenised solution.

Having obtained values for reflectance (R) and transmission (T) of several samples with different thicknesses, a graph of $Ln[(T)/(1-R)^2]$ against d, was plotted for particular wavelengths by rearranging equation 3.16. The absorption coefficient, α, was then found from the gradient of the line.

For the centrifuged samples, the first absorption peak of polyaniline was found at 321nm, which corresponds to the π–π^* transition of the benzenoid structure [9]. The corresponding absorption coefficient is $1.3x10^5 c\,m^{-1}$ obtained from Figure 3.7. For the next absorption peak, at 642nm, which is due to the formation of self-trapped excitons in the quinoid ring, the absorption coefficient is $0.74x10^5 c\,m^{-1}$, seen in Figure 3.8.

It can be seen from Figures 3.7 and 3.8, that as the thickness of the sample increases, the value of $Ln[(T)/(1-R)^2]$ decreases (equation 3.16). Both graphs give reasonably good straight lines. Next, for a single sample of thickness 0.135μm, the absorption coefficient was evaluated and this is shown in Figure 3.9 (using predetermined values of T and R). An almost identical curve was plotted for the sample of thickness 0.180μm which had also been spun from a centrifuged solution. Similar results were recorded for a sample spun onto a sapphire substrate (also 0.180μm thick and prepared by centrifuging) and a sample 0.17μm thick, whose solution had also been homogenised.

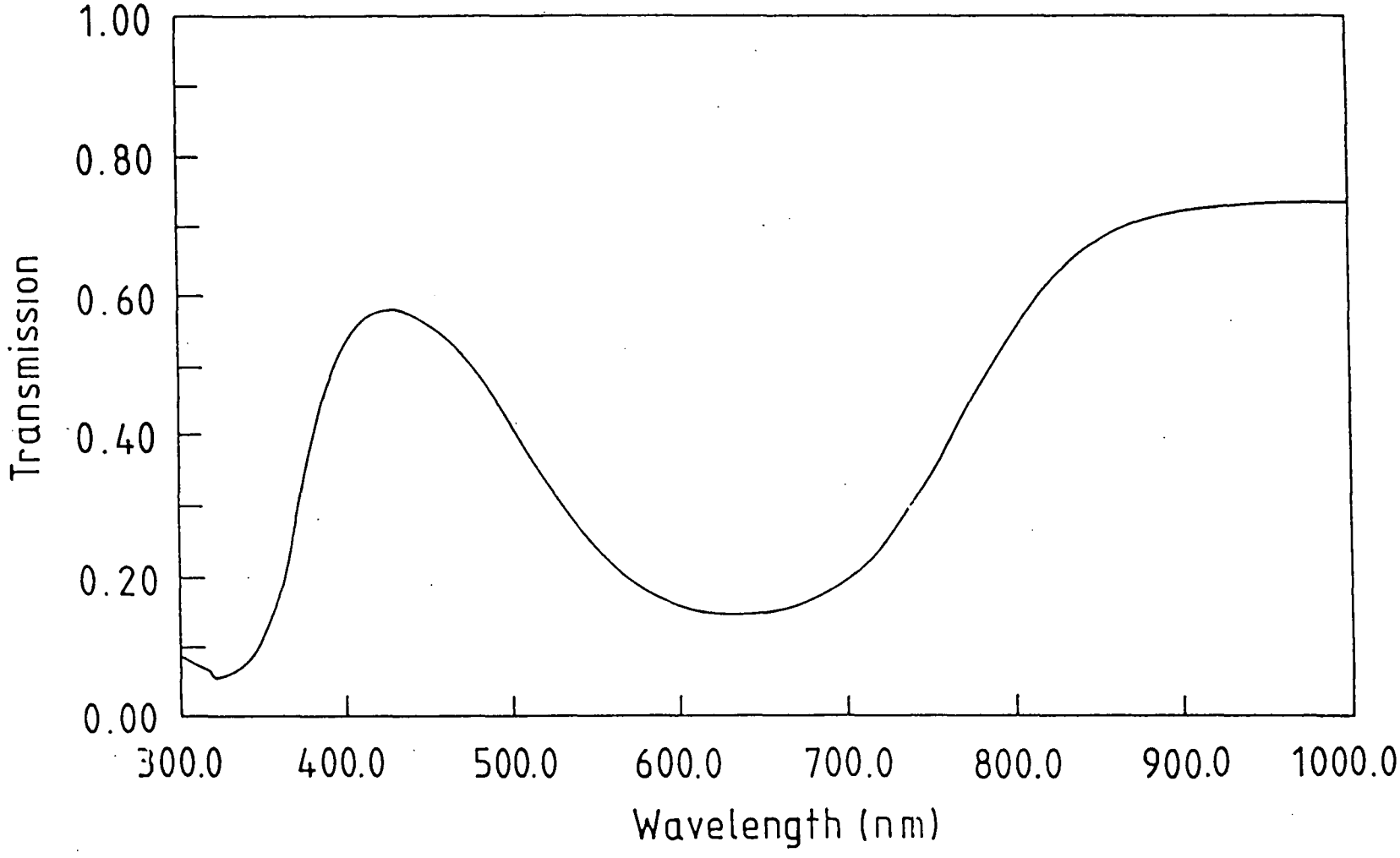

Figure 3.5. A transmission spectrum for a polyaniline spun sample, 0.12μm thick.

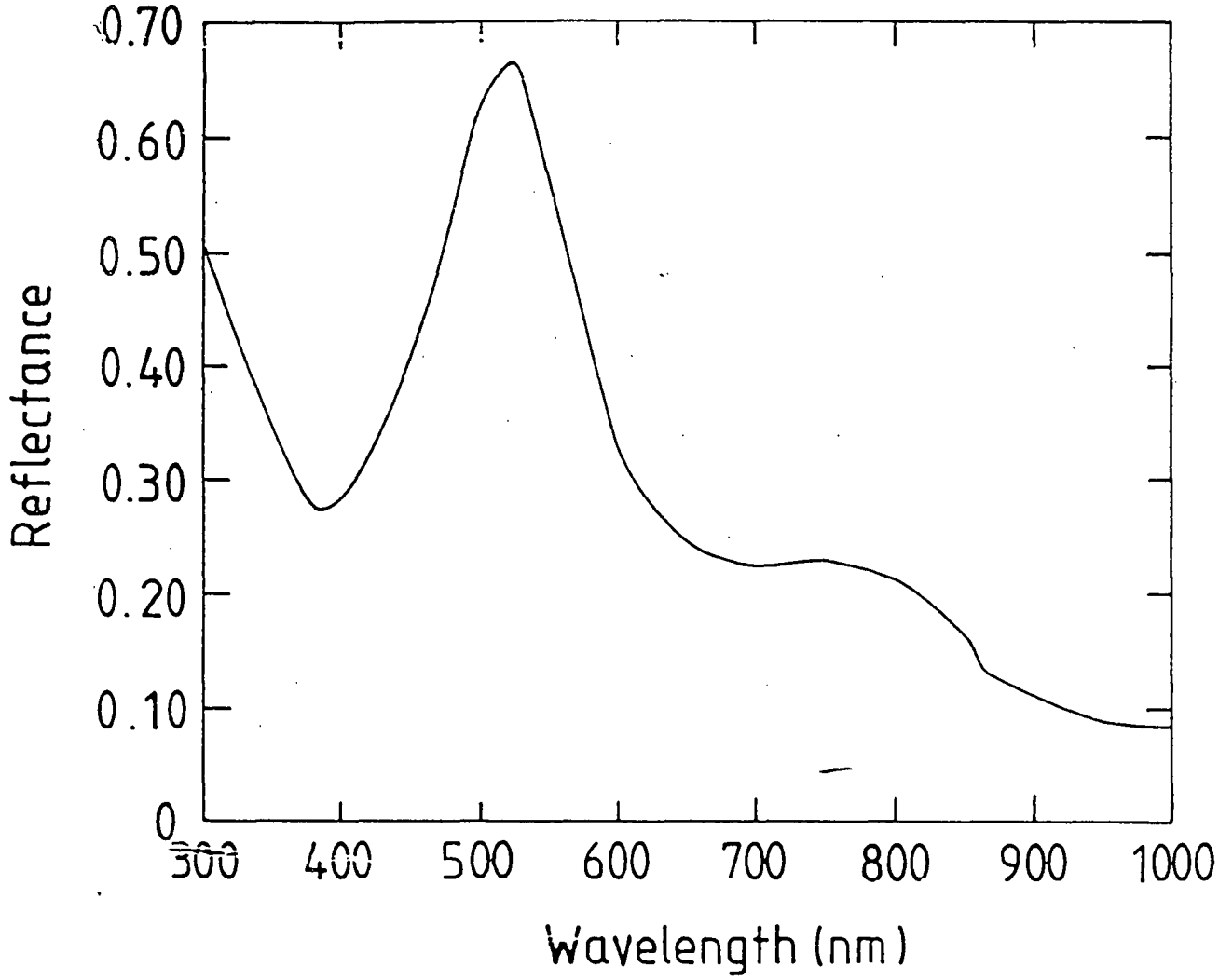

Figure 3.6. A reflection spectrum for a polyaniline spun sample, 0.12μm thick.

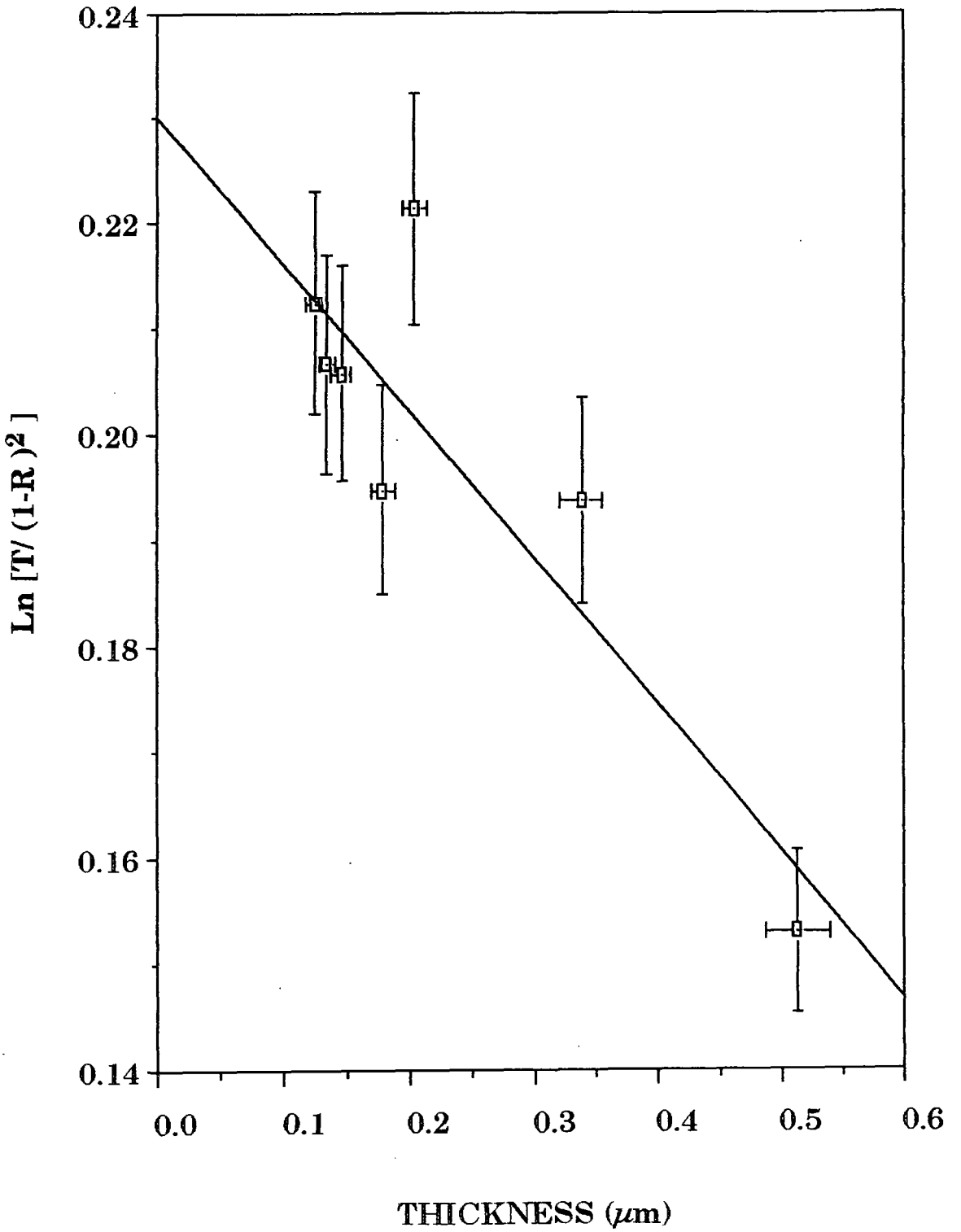

Figure 3.7. Ln[T/(1-R)^2] against thickness, to measure the absorption coefficent of polyaniline at 321nm.

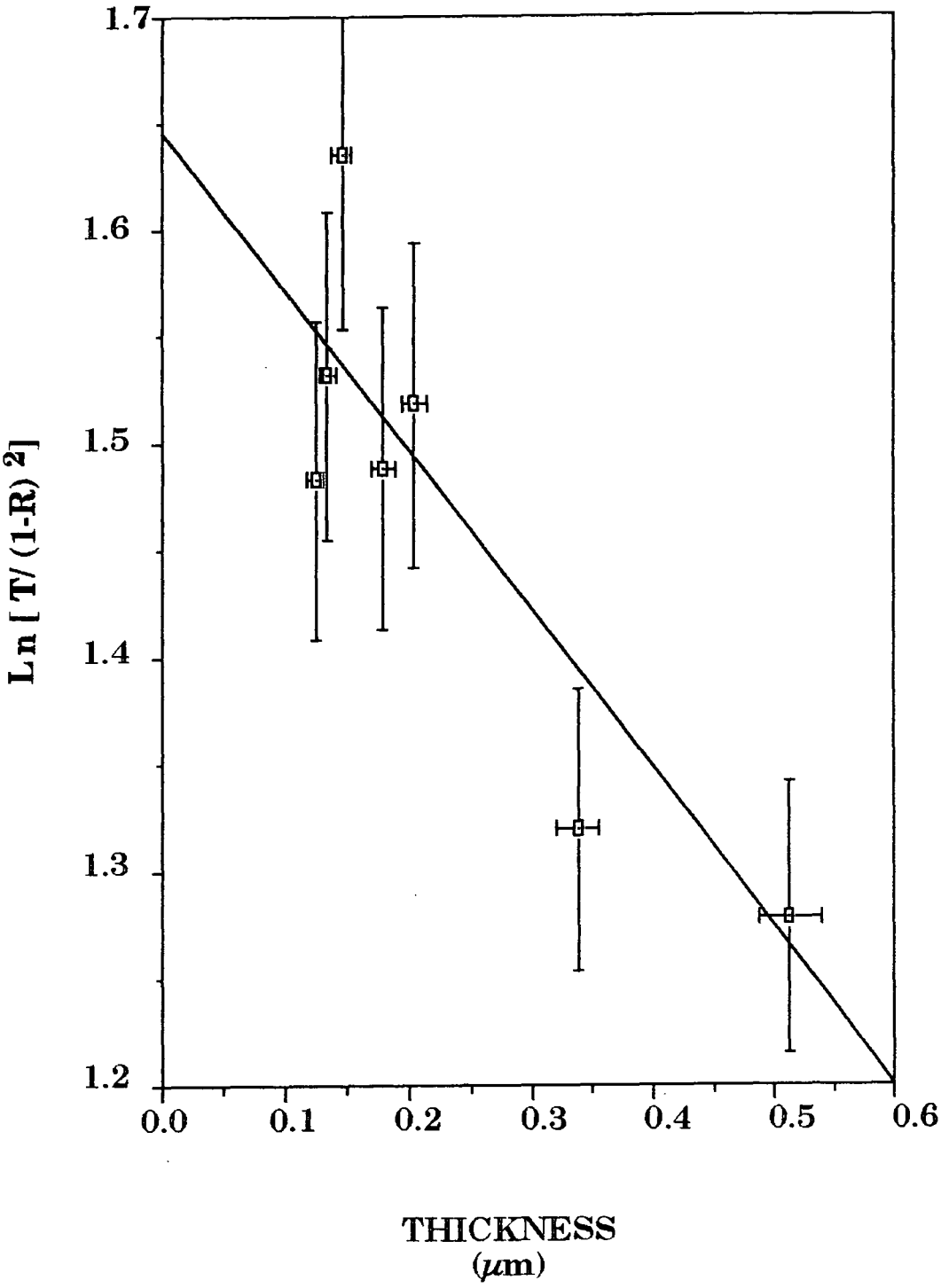

Figure 3.8. Ln[T/(1-R)^2] against thickness,d, to measure the absorption coefficient of polyaniline at 642nm.

Having found the absorption coefficient as a function of energy, corresponding graphs of ($\alpha\hbar w$) against energy were plotted [10], using a similar approach to that for amorphous semi-conductors. By extrapolating, the values of the onset of optical absorption and the optical band-gap, E_g^{opt}, could be found accurately, for deprotonated emeraldine-base polyaniline, according to

$$\alpha(\hbar w) = K(\hbar w - E_g^{opt}) \qquad \ldots 3.17$$

where K is a constant. This is shown in Figure 3.10 for a sample 0.135μm thick, in Figure 3.11 for a sample 0.180μm thick and in Figure 3.12 for a sample 0.180μm thick which had been spun on a sapphire substrate. Accurate band edges have been measured by extrapolating the linear parts on the graphs which correspond to the band onset and three main transitions have been observed.

To explain the semi-conductor nature of emeraldine-base polyaniline, the theory presented by Bredas et al has been used [1]. He proposes a theoretical band structure, which is shown in Figure 3.13. The electronic

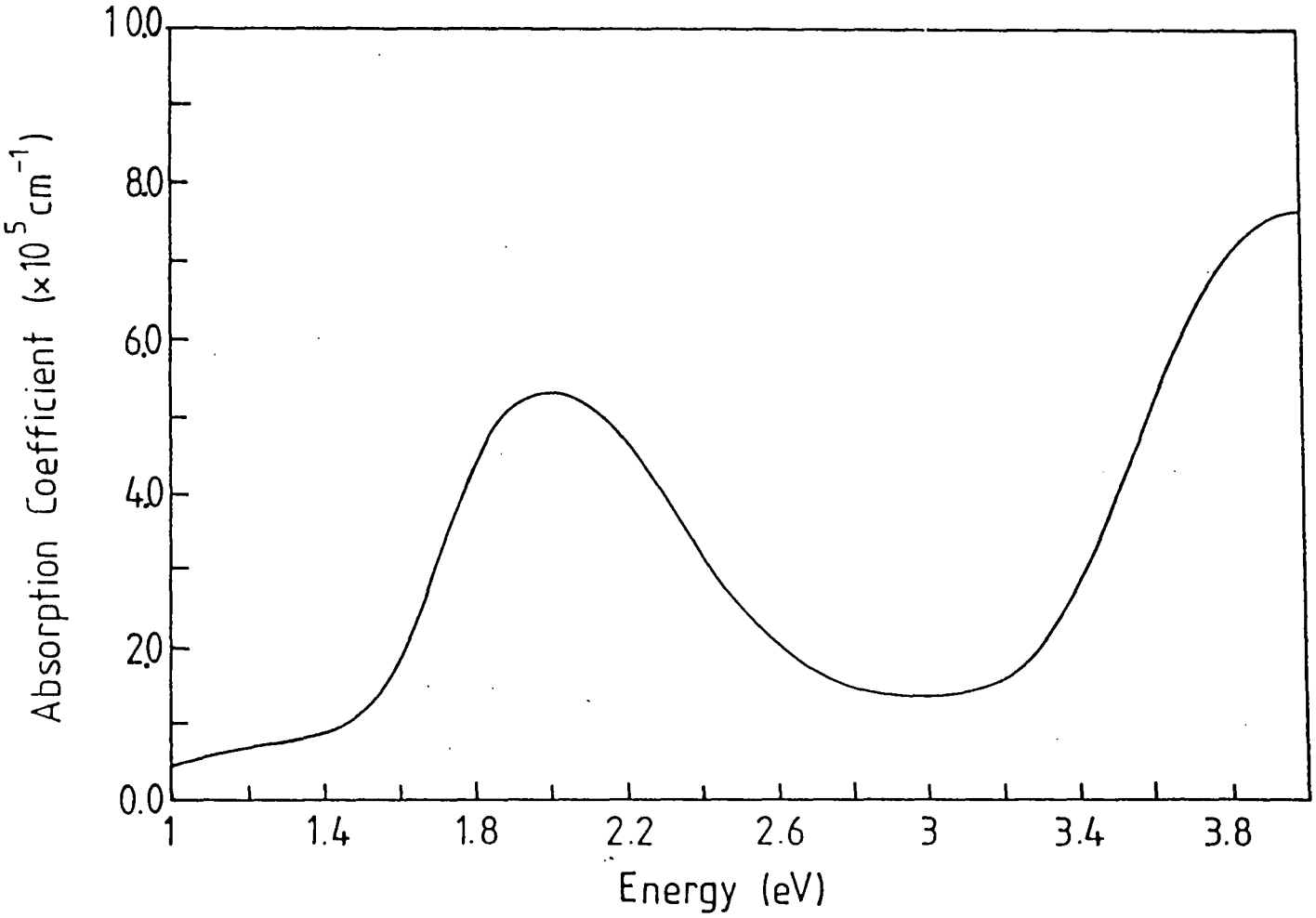

Figure 3.9. The variation of absorption coefficient with energy for a centrifuged solution which has been spun to a thickness of 0.135μm.

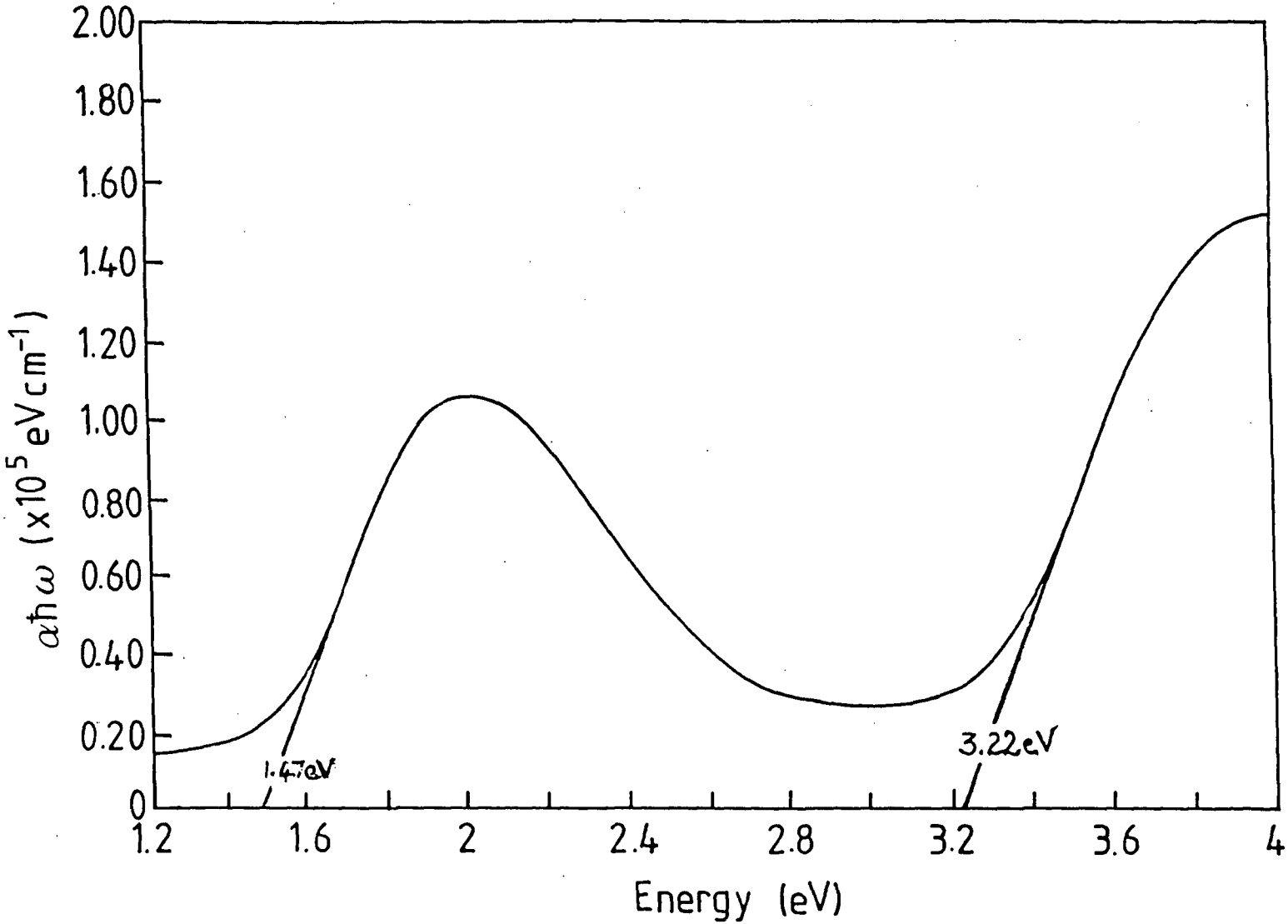

Figure 3.10. The variation of $\alpha\hbar\omega$, with energy for a centrifuged solution which has been spun to a thickness of 0.135μm.

structure has been modelled using a Valence Effective Hamiltonian (VEH) approach. The emeraldine base band structure is predicted to consist of four bands a, a', b and b', as shown on Figure 3.13. The band b' is empty and corresponds to the lowest unoccupied molecular orbital (LUMO). This band is mostly localised on the quinoid ring whereas the other branches derive from the three rings that possess aromatic geometry. The highest occupied molecular orbital (HOMO) corresponds to band b. The band gap is thus the transition given by b - b' and correlates to an energy of 1.4eV.

Our experimental results show that the longest wavenumber feature had a peak value at 620nm, equivalent to 1.47eV and this may be attributed to the theoretical band gap transition of the polymer using the approach of Bredas [1]. Alternatively, if the chain structure is considered as separate quinoid and benzenoid moities, this transition can be ascribed to an exciton formation on the quinoid ring [11]. This is thought to take place during the absorption process when a hole and an electron are formed, giving an exciton. The electron is localised on the imine structure, while the hole is delocalised over the adjacent phenyl structure.

Secondly, the band at 320nm, or 3.22eV can be assigned to a π-π^* transition of the benzenoid units [12]. Using the model of Bredas, this feature probably corresponds to a transition from an occupied level below the valence band, a, to the LUMO, b'. A possible absorption is indicated on the band structure diagram of Figure 3.13.

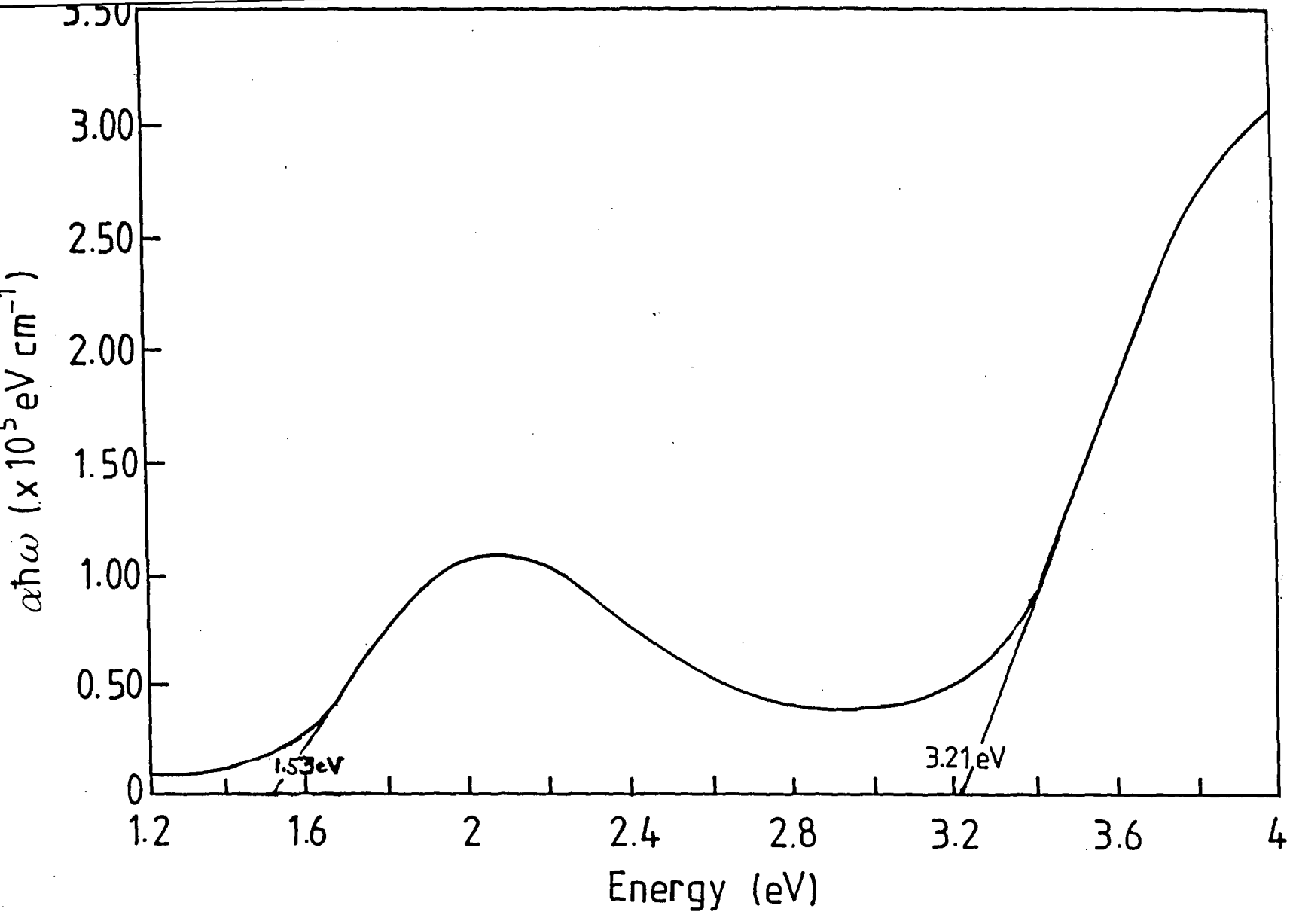

Figure 3.11. The variation of $\alpha\hbar\omega$, with energy for a centrifuged solution which has been spun to a thickness of 0.180μm.

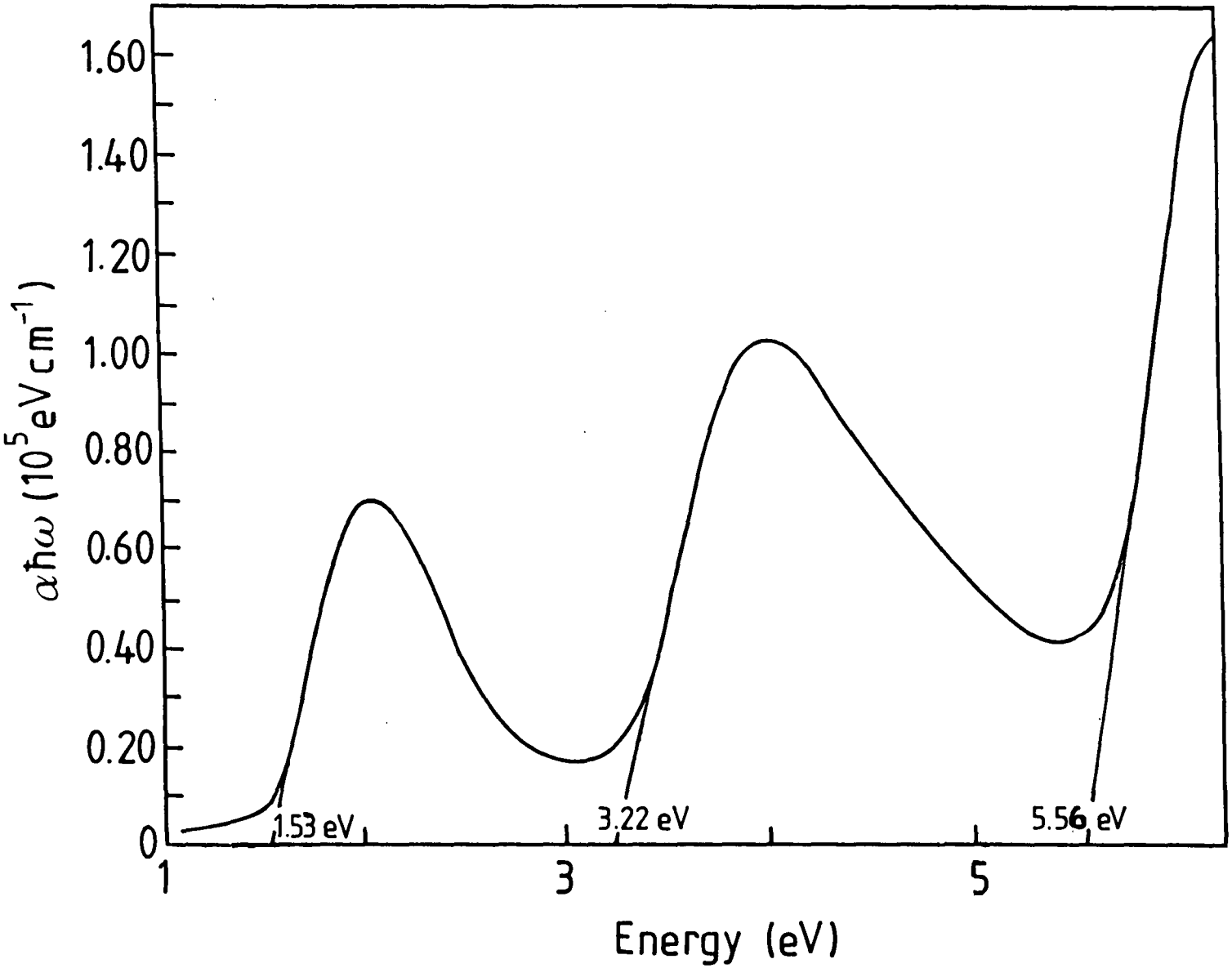

Figure 3.12. The variation of $\alpha h\omega$, with energy for a centrifuged solution which has been spun on a sapphire substrate to a thickness of 0.180μm.

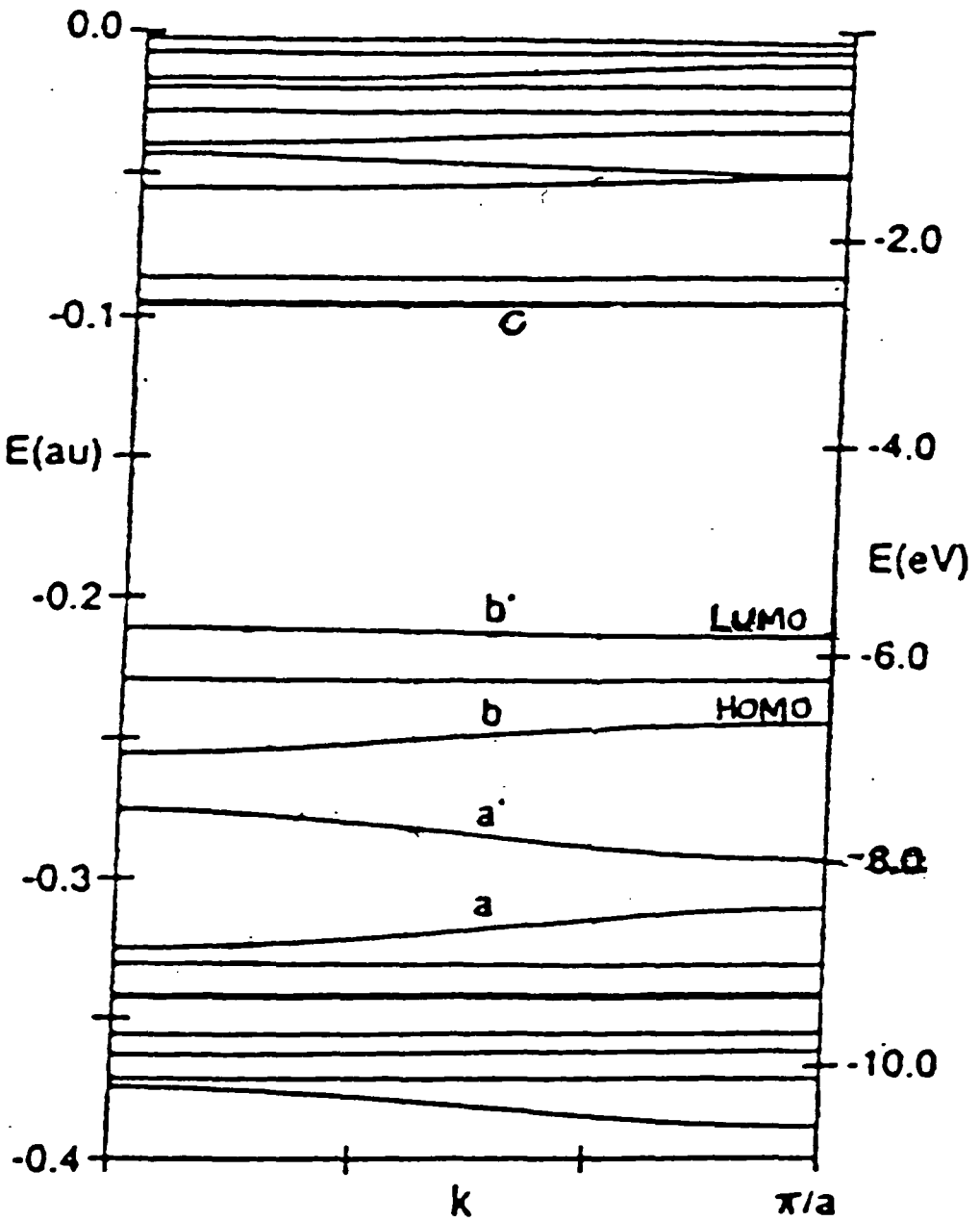

Figure 3.13. Experimental results all measured at the k=0 transition and are fitted to theoretical predictions on the band structure of emeraldine base polyaniline. As a guide to the eye

b - b' = 1.47 eV
a - b' = 3.22 eV
a' - c = 5.56 eV

Finally, a further transition is observed at 183nm (5.56eV). This is a feature which has not been previously reported. As yet, its origin is not fully understood. Clearly though, this absorption corresponds to an energy greater than that of the band gap and as such, must involve bands other than b and b'. A possible transition, roughly equivalent to 5.56eV which compares to the theoretical model is illustrated in Figure 3.13 (i.e. a' - c). The associated experimental evidence suggests this to be a molecular transition in the substituted benzene ring [13].

Table 3.2 compares the onset of absorption corresponding to the three proposed transitions of samples of different thicknesses and whose preparation methods and substrates were varied. It can be seen that the experimental results are in excellent agreement with the theoretical values proposed by Bredas [1].

The slight variations in energy could possibly be due to different thickness of film used and the method of preparation of solution of polyaniline, or even the substrate used.

3.4 Conclusions

It can be seen that by spin-coating a high quality film onto a substrate, the optical properties of polyaniline can be investigated. For deprotonated emeraldine-base polyaniline, the onset of the optical band-gap and other energy bands, due to corresponding transitions have been calculated from experimental work. These prove to be in close agreement with theoretical values reported in the literature [1].

	Energy transition of benzenoid structure. a - b*	Energy transition of quinoid structure. b - b*	Energy transition of benzene structure. a* - c
Theoretical work [1].	3.14eV	1.40eV	6.00eV
0.135μm centrifuged glass substrate.	3.22eV (+/- 0.05eV)	1.47eV (+/- 0.05eV)	
0.180μm centrifuged glass substrate.	3.21eV (+/- 0.05eV)	1.53eV (+/- 0.05eV)	
0.180μm centrifuged sapphire substrate.	3.22eV (+/- 0.05ev)	1.53eV (+/- 0.05eV)	5.56eV (+/- 0.05eV)
0.170μm homogenised glass substrate.	3.18eV (+/- 0.05eV)	1.50eV (+/- 0.05eV)	

Table 3.2 The theoretical and experimental values of the optical band gap, measured at the relevant wavelength.

References

[1] J.L Bredas - 'The Polyanilines' in Proceedings of the Nobel Symposium on conjugated polymers and related materials, Oxford, (1992).

[2] T.S Moss - Optical properties of semiconductors, Butterworth Publications Ltd., (1959).

[3] F.A Jenkins and H.E White - Fundamentals of optics, McGraw-Hill, (1957).

[4] O.S Heavens - Optical properties of thin solid films, Dover Publications, (1965).

[5] K. Chopra - Thin film phenomena, McGraw Hill, 1969.

[6] L.Scheflan and M.B Jacobs - Handbook of solvents.

[7] C.Grovenor - Microelectronic materials, Adam Hilger publications, (1955).

[8] Perkin Elmer - User documentation for the Lambda 19 UV/VIS/NIR spectrometer.

[9] A.P Monkman and P.Adams - Synthetic Metals **40**(1991),87-96.

[10] Mott and Davies -Electronic processes in non-crystalline materials, 2nd edition, Oxford, (1979).

[11] A.Monkman, D.Bloor, GC Stevens, JC Stevens, P.Wilson - Synthetic Metals, **29**(1989)E277.

[12] A.Monkman, J.Bredas and R.R Chance (eds.), - Conjugated polymeric Materials, NATO ASI Series E: Applied Sciences, **182**, (1990), 273.

[13] C.B Duke, E.M Conwell and A.Paton - Chem. Phys. Lett. **131**, (1986), 82

Chapter 4

Polyaniline as a gas sensing material

4.0 Introduction

Several factors have to be considered, before deciding whether to use polyaniline on a commercial basis for gas sensing. Firstly, can it be produced at a reasonably low cost? Can it detect gases at room temperature? Finally, is it a sensor which can be used repeatedly, is reliable and hard-wearing? Although some of these questions still need definite answers, work has been carried out here, the results of which support the argument that polyaniline is important as a usable material for gas sensing [1] in terms of finance and production.

The response of polyaniline to certain gases has been investigated and this chapter presents the results found from exposing polyaniline devices of different thicknesses, to NO_x gas.

4.1 Experiments

The emphasis up until now, on producing high quality polyaniline spun films, is of particular importance for the gas sensing measurements, since lumps or defects in the films can cause irregularities in the sensing results. These high quality films of various, known thicknesses have been used to monitor the delay time in the gas taking effect on the film, the change in current with time (when the gas is present), the time taken for the film to return to its initial state once the gas is switched off and the effect of different concentrations of the gas on the device.

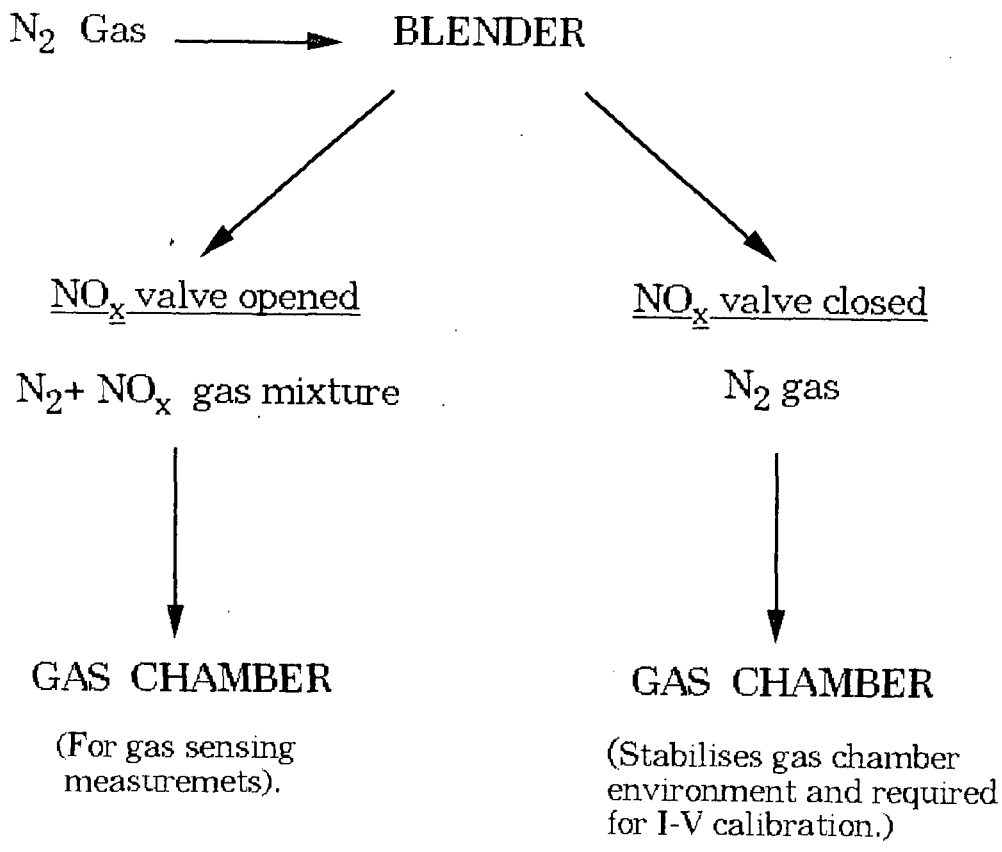

Figure 4.1. A flow diagram showing the experimental method used for gas sensing measurements.

The layout of the system is shown in Figure 4.1. The polyaniline spin-coated device used as the gas sensor was positioned in a gas chamber. A blender controlled the concentration of gas to be passed into the gas chamber and by means of recording changes in current for a fixed voltage across the device, (i.e changes in conductivity) the gas sensor could be characterised for each specific gas concentration. All work was undertaken at room temperature and atmospheric pressure.

4.2 The gas blender

The instrument used in this work was a Signal Instrument Series 850 blender, shown in Figure 4.2.

The blender was connected to two gas cylinders, one being the gas to be sensed, the other being nitrogen carrier gas. The entire system was kept in the fume cupboard, as any leaks could prove harmful. Nitrogen gas was used as a dilutant and as a background calibration. It was passed through the gas chamber continuously, while an experiment was running, keeping the sensor in a constant environment.

The concentration of the gas passed through the gas chamber was controlled by the blender. Utilising a dial on the front of the box and, by consulting a calibration chart the gas concentration in parts per million (ppm) could be programmed.

4.3 The gas chamber

The gas chamber was a sealed unit, as can be seen in Figure 4.3, in which the sensing device was placed. It has been developed in-house at Durham and it ensured that while the gas sensing experiments were being

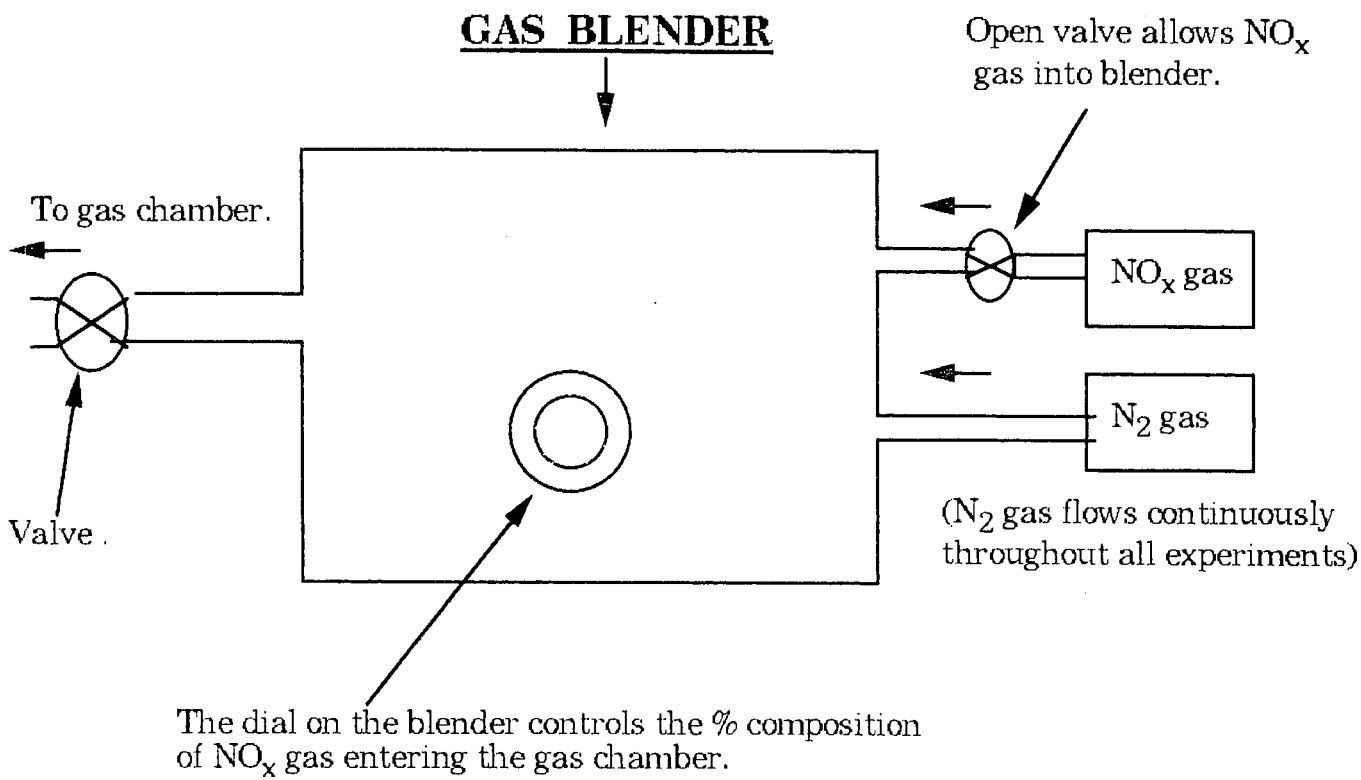

Figure 4.2. The Gas Blender.

THE GAS CHAMBER

(An enclosed unit).

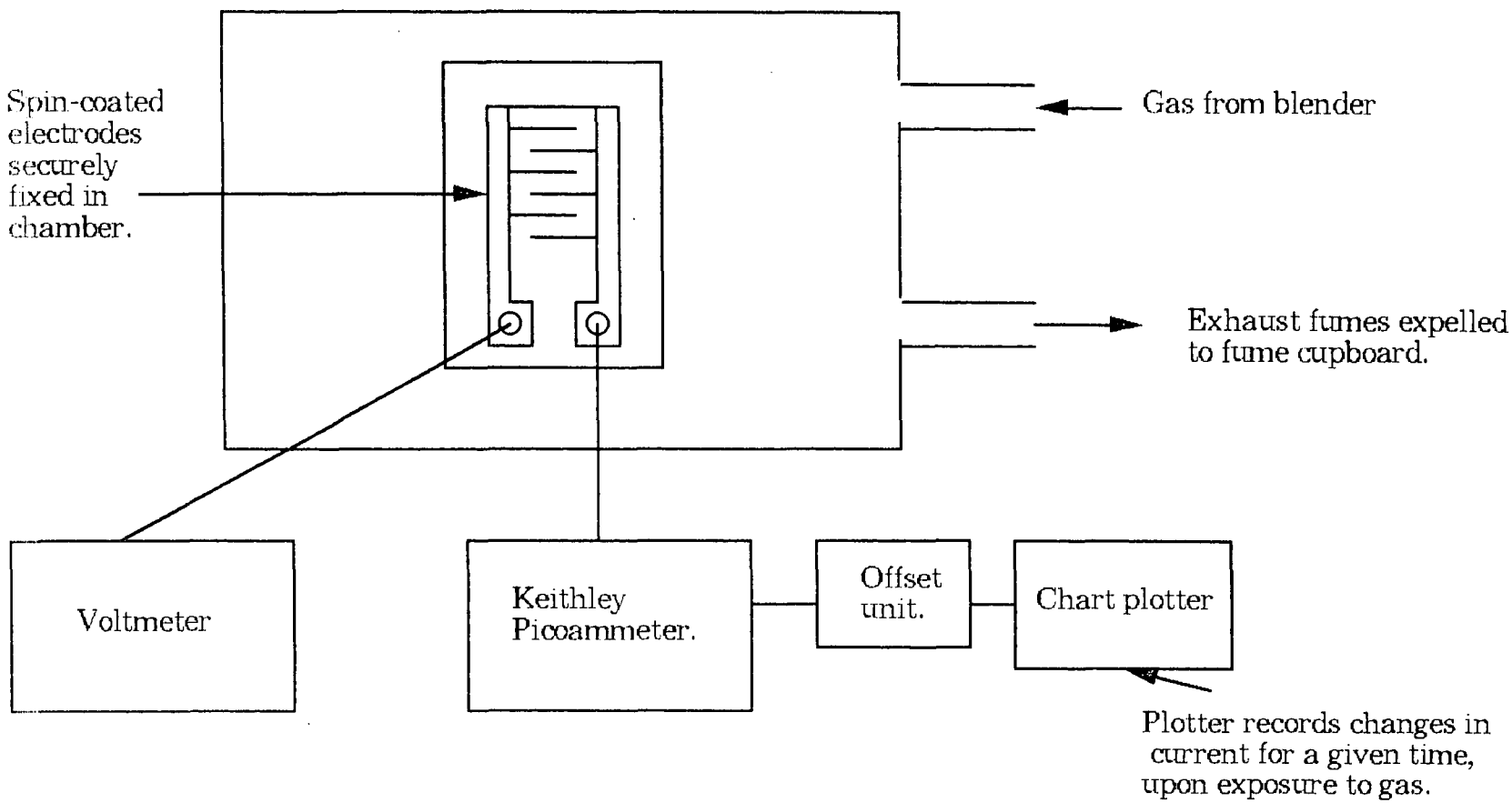

Figure 4.3. The Gas Chamber.

carried out, the conditions were as stable as possible. A tube linked the blender to the chamber and provided the source of gas supply to the device.

An electrical connection was made between the device and gas chamber, using a two-probe metal electrical contact. The device chamber was also connected to a voltmeter and a picoammeter. For a given voltage passed across the device, the change in current was noted over a period of time as the gas was passed through.

4.4 Measurement techniques

For these series of experiments one gas was used, NO_X. NO_X gas (a mixture of nitrogen dioxide and nitrogen oxide gas) is a pollutant produced by cars, power plants and chemical industries. The monitoring of it in the atmosphere has become more and more important recently [2]. Previous work carried out on polyaniline sensors, (using NO_X) has found a highly sensitive device response, of a reversible nature after the NO_X gas had been removed [1].

Interdigitated electrodes (supplied by British Gas which were made by depositing gold on silica, as is shown in Figure 4.4), onto which polyaniline was spun, formed the gas sensing device. Device fabrication was carried out in a clean room environment. The polyaniline solutions were of a 5% concentration, which had been left for 48 hours before being centrifuged three times (and decanted each time). Then, they were spun onto the interdigitated electrodes at 500rpm, 1500rpm and 3000rpm, using the spinning conditions stated in Table 4.1. The electrodes on the device were placed 50μm apart, giving a large surface area.

A device fabricated with a known thickness of polyaniline was then clamped in the gas chamber so it could not move (ensuring reproducibility of the area of exposure throughout the sensing process for each device).

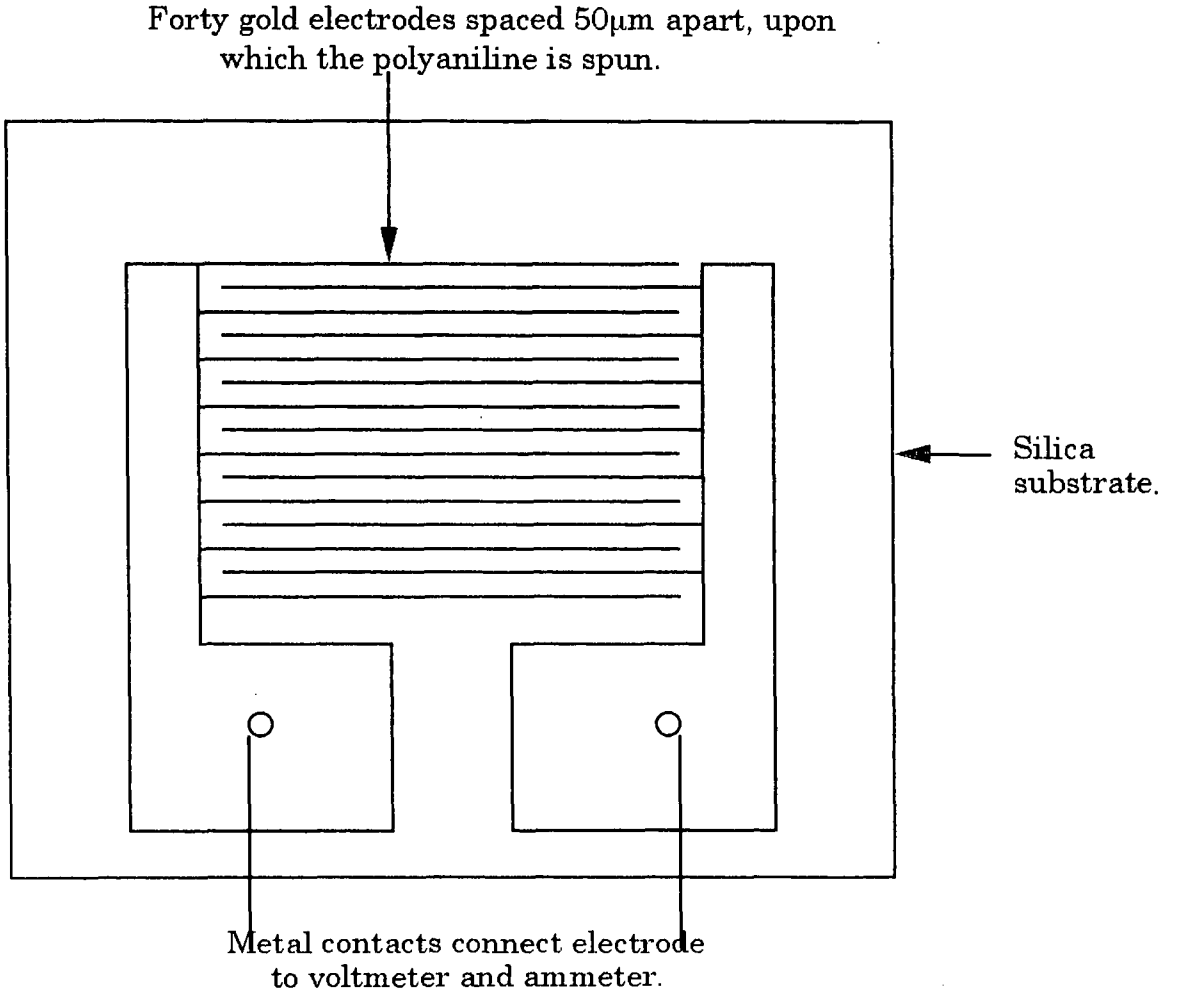

Figure 4.4. This shows the interdigitated electrodes used for the gas sensing experiments.

Contact was made between the device and the chamber, (as can be seen in Figure 4.4), by two pressure contacts inside the chamber. To remove the polyaniline on the electrodes which enabled a good metal-to-gold contact, NMP was gently rubbed over the contact area. Initially, an interdigitated electrode which had not been covered with polyaniline was used as a control.

The current in both forward and reverse bias was measured, for different applied voltages. Nitrogen gas was then passed through the chamber and a small, fixed voltage of 20mV was applied across the device. A chart recorder was used to record any changes in current.

Speed (rpm).	Time (seconds).	Acceleration (units).
$v_1 = 570$	$t_1 = 60$	$a_1 = 10$
$v_2 = ***$	$t_2 = 60$	$a_2 = 100$
$v_3 = 230$	$t_3 = 60$	$a_3 = 10$
		$a_4 = 10$

v_2 is either 500, 1500 or 3000rpm.

Table 4.1. The spinning conditions used for gas sensing.

Initially, when passing nitrogen gas through the gas chamber, there was a large change in current (due to the removal of residual water from the polyaniline) but this began to stabilise after two minutes. The device took approximately one hour to stabilise fully in the nitrogen gas environment and this was apparent by the chart recorder no longer showing a change in current. The device was then ready to begin the gas sensing experiments

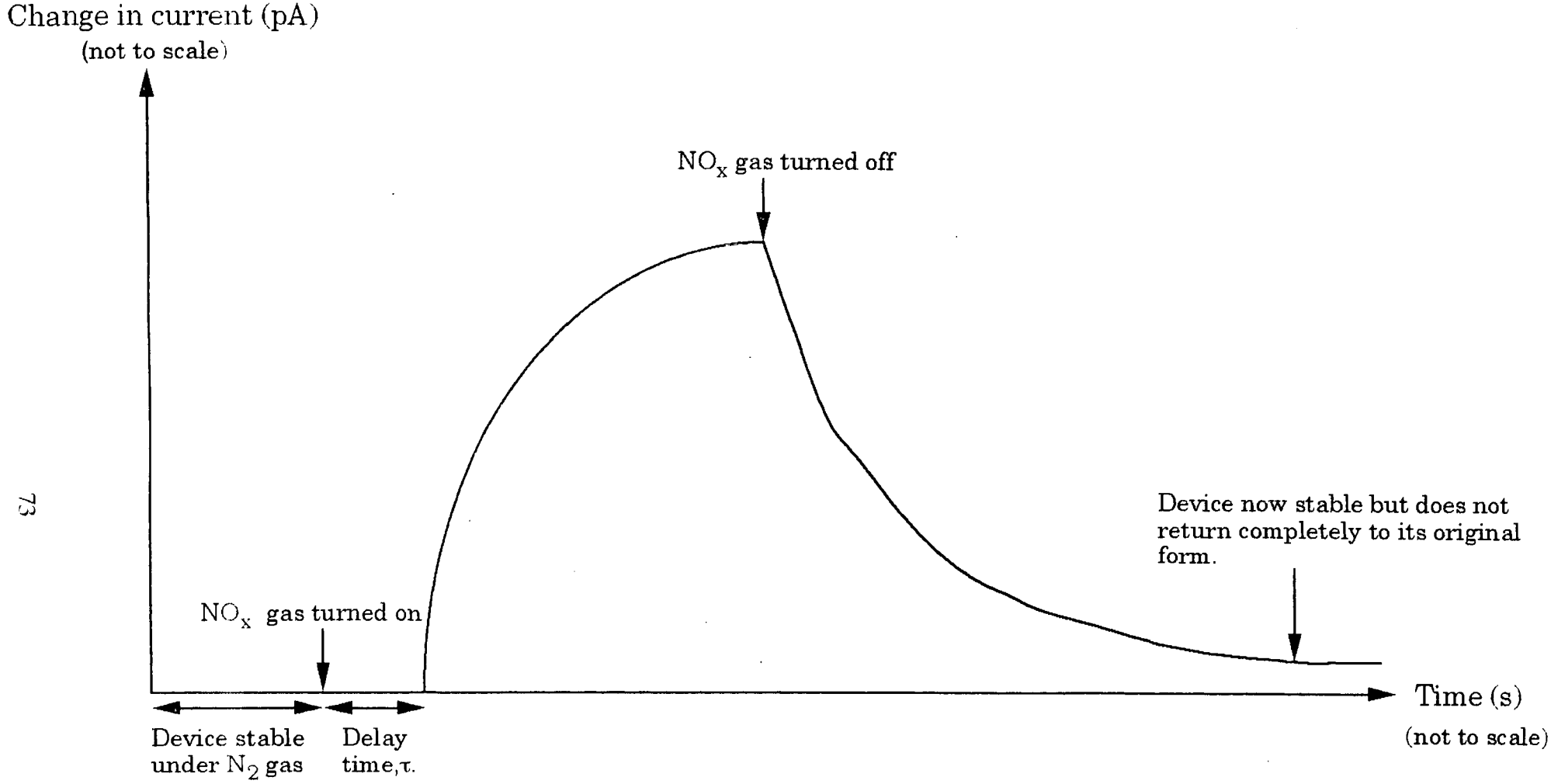

Figure 4.5. A typical NO_x gas exposure plot.

and a typical exposure plot can be seen in Figure 4.5. The device was assumed to be 'undoped' at the start of the experiment.

The initial change in conductivity of the device which was quite large, (shown in Figure 4.5) can be attributed to the NO_x gas reacting with the polyaniline layer. It has also been suggested that the change in conductivity is due to the removal of water molecules, which are trapped in the film [1]. The delay time, τ, was a possible indication of the length of time it took for the gas to travel along the tube, reach the gas chamber, diffuse into the film and react with it.

Once all of the gas sensing experiments had been completed, the thickness of polyaniline deposited on each interdigitated electrode was measured, using a Tencor 100 Alpha step. Also, the surface area covered by polyaniline was measured using a micrometer screw gauge.

4.5 Results

(a) Ohmic contacts

For the interdigitated electrode without a polyaniline layer, there was no measurable change in current on increasing the voltage. This indicated the relatively high resistance of the silica substrate.

Applying an even, lump-free layer of polyaniline to cover the interdigitated electrode completely and repeating the two-point conductivity measurements in nitrogen gas, the current versus voltage behaviour indicated good Ohmic contacts for all three devices. Figure 4.6 shows these results (for the devices spun at 500rpm, 1500rpm and 3000rpm). The current-voltage measurements were also repeated after exposure to the NO_x gas and these also showed Ohmic behaviour, indicating good contact had been kept throughout the experiments.

(b) Resistivity measurements

For a conducting material, it is known that,

$$\rho = \frac{1}{\sigma} = \frac{RA}{x} \qquad \ldots 4.0$$

where σ = conductivity ($\Omega^{-1}m^{-1}$).

ρ = resistivity (Ωm).

A = cross section area of layer (m^2).

x = distance between adjacent electrodes (m).

R= resistance of the polyaniline thin film (Ω)

and this is represented diagrammatically in Figure 4.7.

Using this relation, the change in current with voltage can be plotted and the resistance, R, of each polymer sample can be found from the gradient of the graph, in Figure 4.6. Here, it is assumed that the resistance of the polymer is measured and not the contact resistance between the electrodes and the film.

The value of the cross-sectional area, A, can be calculated easily by knowing the thickness of the device, as can be seen from Figure 4.7. Table 4.2 summarises the results for each device and from this it is clear that sample thickness and resistivity decrease with an increase in spin speed. The resistivity of the devices 0.19μm and 0.09μm thick are very similar, which implies a uniformity between their fields. Since there is a slight difference in the resistivity of the thicker device (1μm thick), this shows there must be a difference in uniformity of the field, with respect to the other two device. Although the dimensions of the electrodes (especially the height of the fingers) are not thought to effect these results, this is certainly an area for further study.

(c) Delay time

The delay time, τ, as shown in Figure 4.5, is the time between the NO_x being switched on and for a change in current to register (for a given voltage), corresponding to the gas reacting with the device. This delay time comprises of the time for the gas to travel down the pipe and the time taken for it to react with the device.

Device spun at:-	d (μm)	x (μm)	A (cm^2)	R (Ω)	ρ (Ω cm)
500rpm	1.00	50	1.0×10^{-4}	5.4×10^{9}	1.1×10^{10}
1500rpm	0.19	50	1.9×10^{-5}	1.1×10^{10}	4.2×10^{9}
3000rpm	0.09	50	9.0×10^{-6}	1.2×10^{10}	2.2×10^{9}

Table 4.2. This table compares the resistivity, conductivity and surface area of the three devices, of different thickness, d, which have been spun at different speeds.

It has been found that nitrogen gas could take up to two minutes to leave the gas cylinder, travel along the connecting tubes to the gas chamber where it then interacted with the device (changing its resistance). However, NO_x took on average, one minute to travel along the gas chamber and register a change in current. As gas flow for both gases will be approximately the same, NO_x gas must therefore react more quickly with the polymer films.

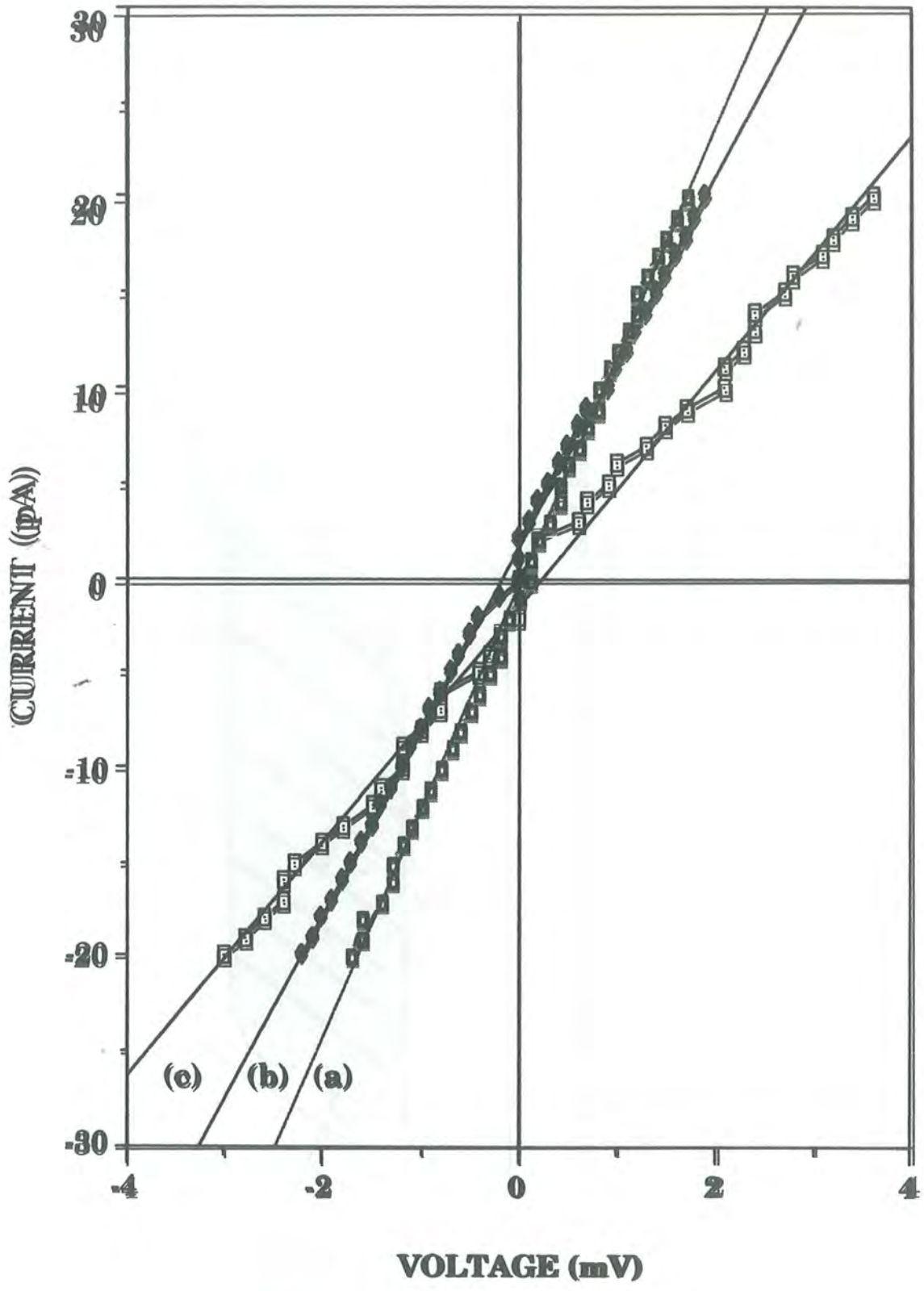

Figure 4.6. Current versus voltage for three devices spun at (a) 500rpm,1.0μm (b) 1500rpm, 0.19μm (c) 3000rpm, 0.09μm.

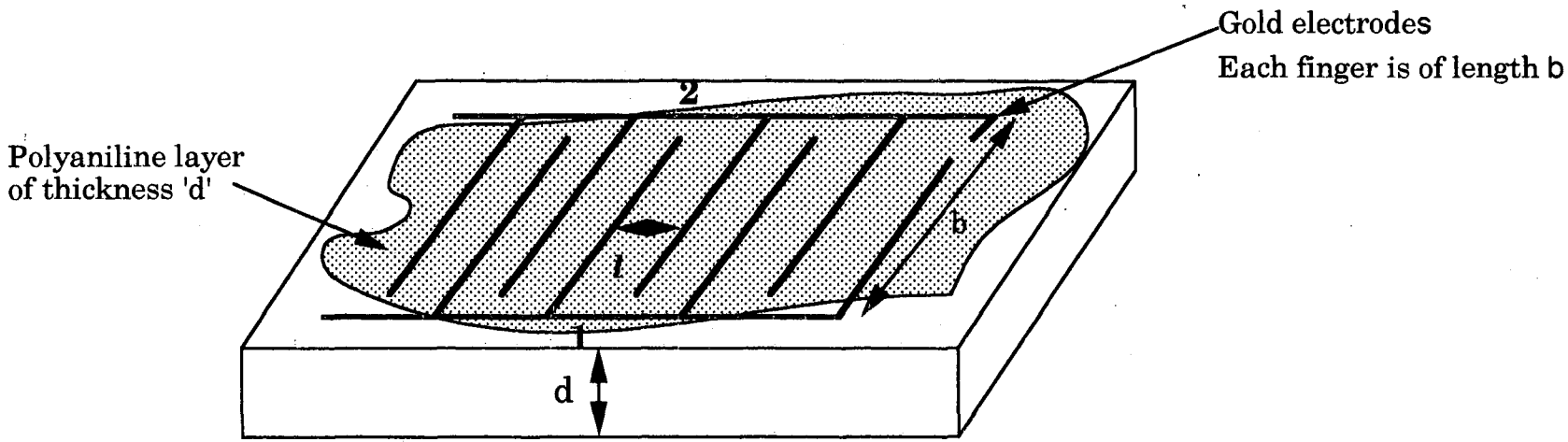

A potential difference is measured between points **1** and **2**, for a fixed current (to give a value for the resistance, R,of the polyaniline film).
l is the distance between two adjacent electrodes.
The cross sectional area, A, is calculated by multiplying d by b.
b is of length 1cm
d is the thickness of the film

Figure 4.7. The arrangement for conductivity measurements.

Table 4.3 shows the variation of delay time for each given concentration of NO_x gas exposed to each polyaniline device at room temperature. A general trend shows that the lower gas concentrations take longer to produce an effect. However, with thinner polyaniline-film devices (i.e spun at a higher speed), it can be seen that the delay time is less, even when exposed to a low gas concentration. This implies that the thinner the active layer on the device, the more sensitive it is to NO_x gas.

Film thickness	1.000μm (500rpm)	0.185μm (1500rpm)	0.085μm (3000rpm)
Concentration of NO_x gas (ppm)	Delay time (τ) / Seconds.		
10	144	72	72
20	120	84	72
30	96	72	60
40	72	72	48
50	60	60	48
60	72	60	48
70	60	50	48
80	60	48	48
90	60	48	48
100	48	48	48

Table 4.3. The variation in delay time for NO_x gas to register with the three polyaniline devices (which have been spun at different speeds).

(d) Changes in conductivity upon exposure to NO_x gas

(i) The change in current with time.

Figure 4.8 shows a graph of the change in current as a function of time, for five different concentrations of NO_x. The results are from the polyaniline device which has been spun at 1500rpm and they show that the device produces a lower resistance change when sensing lower concentrations of the gas. This result is in agreement with previous experiments [4].

For a low concentration of NO_x (20ppm), the data points show a lot of scatter. However, as the concentration is increased, the change in current becomes more regular. Also, at higher concentrations after approximately three minutes of exposure to NO_x gas, the change in current with time becomes more linear.

(ii) The change in current with time for three devices, measured at the same gas concentration.

The variation of current with time for the three devices at a NO_x gas concentration of 50ppm are plotted in Figure 4.9. Several points can be made about these results. Firstly, it can be seen that a thicker polyaniline device (500 rpm, 1.0μm) shows a much smaller change in current than do the devices spun at 1500 rpm (0.185μm) and (3000 rpm, 0.085μm), for the same gas exposure.

Secondly, the thicker device (spun at 500rpm) shows a lot of irregular scattering amongst its data points. This implies that the gas reaction is a surface phenomena and that the thicker film effectively shields the surface layer from the electrodes underneath.

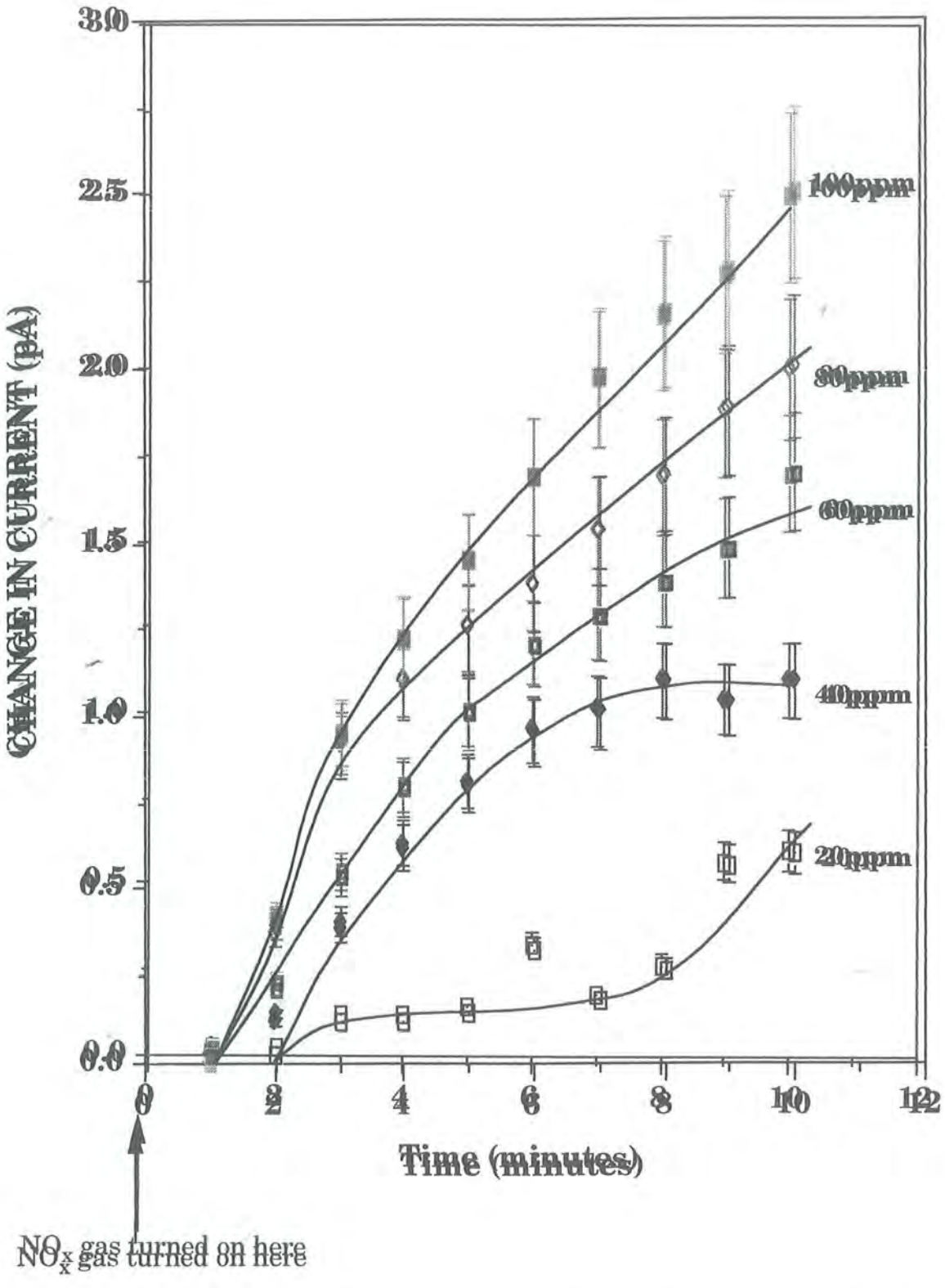

Figure 4.8. The change in current with time for an increase in NO_x concentration, for the device spun at 1500rpm (0.185μm).

Thirdly, the thinner devices (spun at 1500rpm and 3000rpm) show a similar shape on the graph. The thinnest (3000rpm) saturates after five minutes, but the device spun at 1500rpm takes ten minutes to saturate.

(iii) The change in current after five minutes with concentration, for each sample.

Figure 4.10 shows the results for each device taken after five minutes. The thickest device shows a smaller change in current as the concentration of NO_x gas is increased, than those measured for the thinner polyaniline devices (the 3000rpm device showing the greatest change). Therefore, the thicker device is less sensitive to NO_x gas than the two thinner devices. The thicker device also behaves quite erratically when increasing the gas concentration, which is not a particularly desirable feature for practical gas sensors. Such results suggest that the gas reaction is confined to a thin surface layer.

It is interesting to note the similar graph-shapes of the two thinner devices. These suggest a more reliable sensor.

Clearly, it is difficult to monitor a change in current for all of the devices when exposed to NO_x gas, with concentrations less than 10ppm. This must define the limiting sensitivity, which should be taken into account when using polyaniline for gas detection purposes.

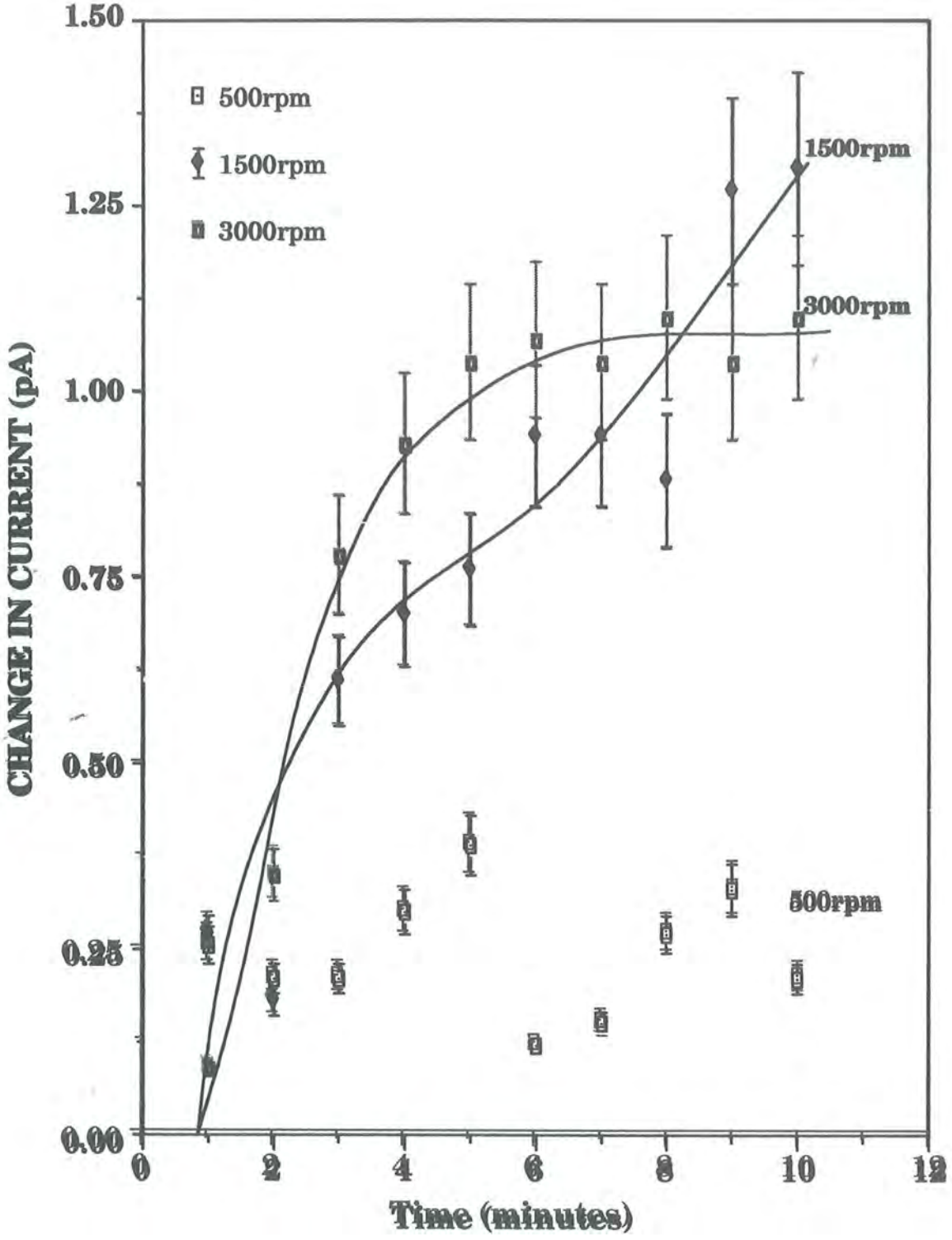

Figure 4.9. The change in current with time for three devices, using an NO_x gas concentration of 50ppm.

(e) Recovery time

The recovery time or reversibility, is an important feature for a reliable gas sensor [5]. It is the time taken for the chemical reaction, which occurs on the surface of the sensor upon exposure to a gas, to recover in such a way (when the gas is removed) that the sensor no longer shows a change in current, for an applied voltage.

For each device, the recovery time as a function of NO_x concentration was measured from the paper plots, by finding the time it took (once the gas had been removed from the device) for the device to no longer show a change in current. A graph showing the results is presented in Figure 4.11. From this graph it can be seen that the thinnest device took the least amount of time to recover.

Increasing the concentration of NOx gas, it can be seen that the recovery time for all devices increases up to a concentration of 50ppm. This suggests that the gas may not have penetrated throughout each film and also that the corresponding reaction has occured on the surface of the film. However, for the device spun at 3000rpm (0.085mm thick), the recovery time decreases when exposed to gas concentrations higher than 50ppm. It is possible that the gas has reacted in a more permanent way with the device, or maybe that the gas has saturated the device at concentrations greater than 50ppm (and so for concentrations greater than this, a true rate of recovery cannot be measured).

The devices spun at 1500rpm (0.185μm thick) and at 500rpm (1μm thick) show a consistent increase in recovery time with an increase in the percentage of NO_x exposed, as expected.

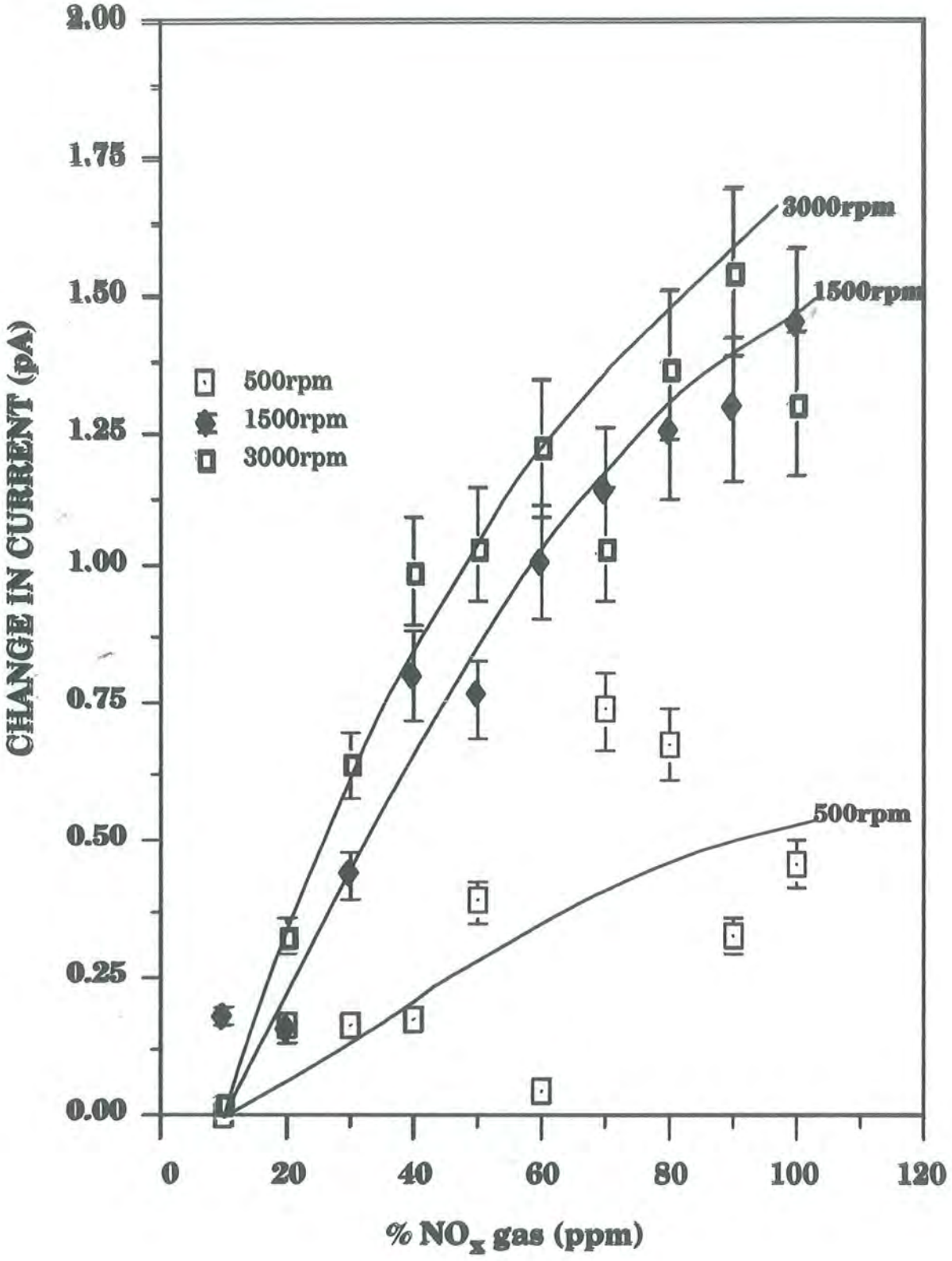

Figure 4.10. A change in current with % concentration of NO_x gas for each device (of known thickness), measured after 5 minutes.

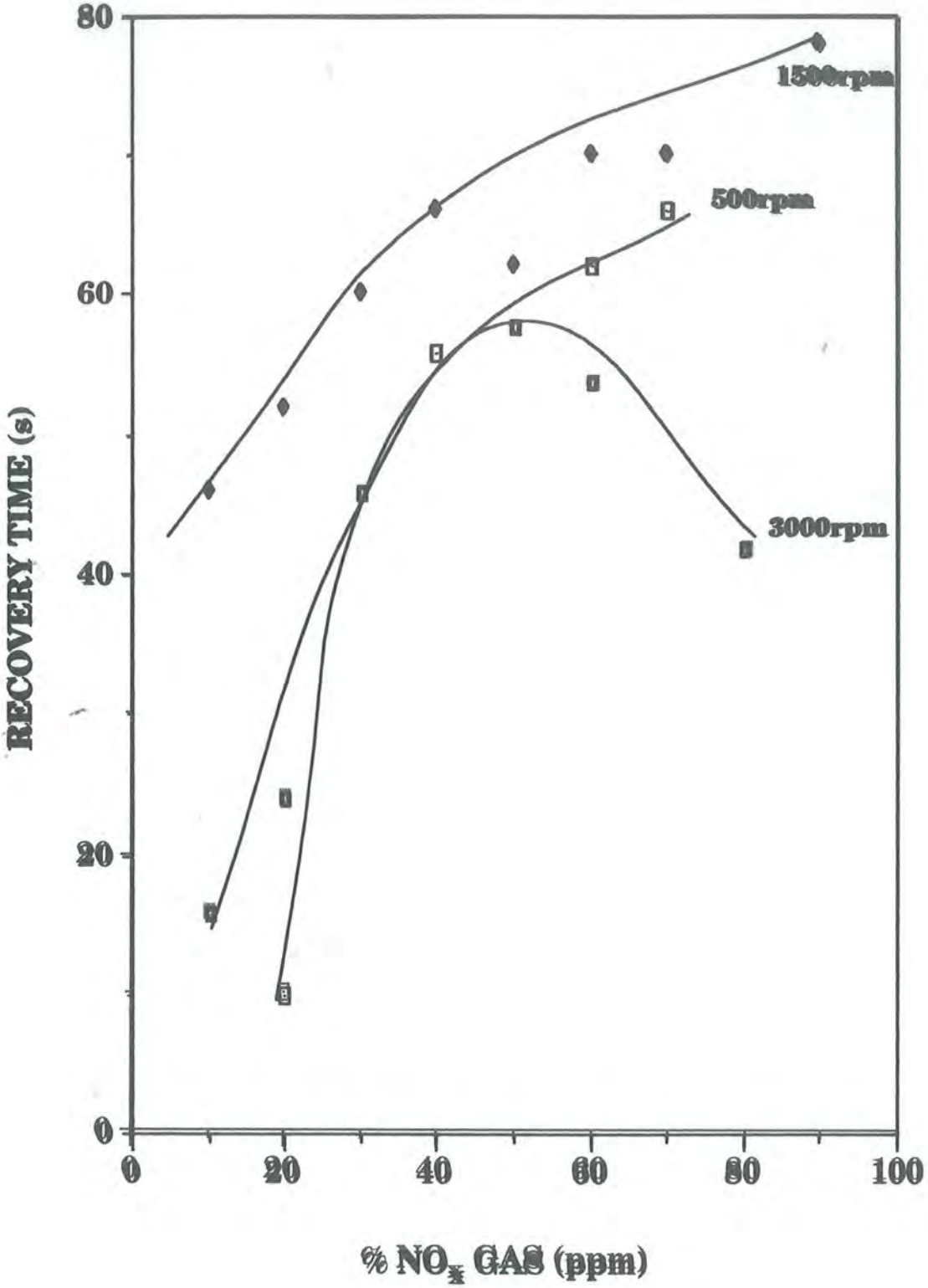

Figure 4.11. The time taken for each device to recover after exposure to each % concentration of NO_x gas.

4.6 Discussion

It can be seen that when the polymer device comes into contact with NO_x gas, there is a change in conductivity. Therefore, it can be concluded that there has been some sort of surface reaction which has the effect of changing the electrical properties of the thin film.

Gopel [5] suggests that changes in electrical properties are due to chemisorption, whereby selective bonds on the substrate undergo a reaction. Further work has suggested that NO_x gas protonates polyaniline [6], [7]. and this is thought to be responsible for the change in conductivity.

The results can be explained in terms of the surface phenomena of the gas interaction. The delay time, τ, is less for the thinner films. As NO_x reacts with more electrons on the imine sites of the polyaniline film (as there will be more readily available), this will register a change in conductivity. This is in effect, doping, which is analogous to protonation. For a thinner film, it will register a change more quickly than for a thicker film, which acts as an effective shield between the surface layer and the electrodes underneath. The effect of current with time for the three devices exposed to NO_x gas must be considered further.

It can be seen that none of the devices, regardless of thickness etc., are sensitive to concentrations of NO_x gas below 10ppm. It is possible that some reaction is taking place at the surface, but the change in conductivity is too small to register. This is an important consideration to be taken into account if the material is to be used as a sensor on an industrial scale.

It should be mentioned here that when plotting graphs of current versus time for each device at a given concentration, there is a lot of scatter amongst the data points. This could be attributed to the quality of the films. Although relatively lump-free, there are still some surface defects present, which can be seen on a microscopic scale (See Chapter 2). It is clear that

these are undesirable, especially in thinner films, where surface defects can result in bulk impurities (due to diffusion). This can influence the sensor properties as the bulk defects can be the cause of irregularities in the sensing experiments [8].

4.7 Conclusions

It can be concluded that polyaniline behaves as a good gas sensor when exposed to NO_x gas, due to a change in its conductivity. Although the device spun at 3000rpm (0.085μm) appeared to be the most sensitive to exposure to NO_x gas, it was found to saturate quite easily. However, the device spun at 1500rpm (0.185μm) proved to be the more predictable and reliable of the three. The change in conductivity upon exposure to NOx gas is due to chemical changes on the surface and the ability to detect these changes depends on the film thickness.

No attempt has been made to model the gas sensing data in terms of a diffusion process, but this is certainly an area for further work.

References

[1] N.E Agbor - PhD Thesis, University of Durham, (1993).

[2] A.Heilmann and M.Miller _ Sensors and Actuators B, 4 (1991)511-513.

[3] H.E Endres and S.Drost - Sensors and Actuators B, 4 (1991)95-98.

[4] N.E Agbor - First year PhD report, Durham University (Unpublished).

[5] Wolfgang Gopel - Sensors and Actuators B, 4 (1991)7-21.

[6] N.E Agbor, M.Petty, M.Scully, A.Monkman - Patent Application No. UK/9300560.1/1993.

[7] Wu-Song Huang, A.G. MacDiarmid, A.J. Epstein - Journal of the Chemical Society, Chem. Common, in press.

[8] C.Grovenor - Microelectronic Materials, Adam Hilger publications, (1955).

Chapter 5

Conclusions and suggestions for further work

5.0 Introduction

In the following chapter the results of the preceding chapters have been summarised. Also at the end there are some suggestions for further work.

5.1 Conclusions

A suitable solvent, NMP (N-methyl-2-pyrrolidone), has been used to dissolve the polyaniline powder, giving a dark blue solution. It has been found that the best solution to work with was made up of 5% weight of polyaniline to NMP. This was left in solution for forty-eight hours, before either being centrifuged three times (each time using the solution which had been decanted off the top), or homogenised. Both techniques provide excellent ways for making up a lump-free solution.

The lump-free solution could be spun onto a thin, circular glass substrate, which had previously been immersed in isopropanol for twelve hours in an ultrasonic bath, before being dried off using nitrogen gas. This process helped improve the final quality of the spun film, leaving it virtually lump and defect free.

The spinning conditions could be altered on the spinner, by means of a programming unit. The spinner itself had an attachment which could heat the film as it was spinning and tests carried out showed that the best temperature to use this at, was 120°C. By the end of the spinning process, which took up to 3 minutes, a thin dry film could be spun which was ready

to use for further experiments. The heater helped to improve the quality of the spun film.

The behaviour of polyaniline as a Newtonian or a non-Newtonian fluid has been discussed and although the results were inconclusive, it has been suggested that during the spinning process, polyaniline goes through phases where it behaves as both a Newtonian and a non-Newtonain fluid.

The thin films were used to investigate optical properties of emeraldine-base polyaniline. By measuring transmission and reflection spectra for several thin films (of different thicknesses, which had also been processed in different ways) and by using the Beer-Lambert law, the absorption coefficient could be measured at a given wavelength. At 321nm, the absorption coefficient was measured to be $1.3 \times 10^5 c\,m^{-1}$ (corresponding to the π-π^* transition of the benzenoid structure), and at 642nm, the absorption coefficient was $0.74 \times 10^5 c\,m^{-1}$ (corresponding to the formation of self-trapped excitons in the quinoid ring).

Following on, the optical band gap, E_g^{opt} could be measured and was found to have a value of approximately 1.5eV. An energy transition corresponding to the π–π^* transition of the benzenoid structure was found to be at about 3.2eV, and a transition at approximately 5.6eV was thought to be a molecular transition in the substituted benzene rings along the polymer backbone. These results are in agreement with theoretical predictions [1] and other experimental results [2].

Having improved the quality of the thin films, so they were virtually defect and lump free, thin films of controlled thickness were spun onto gold electrodes. These were exposed to different concentrations of NO_x gas and changes in current for a given voltage were monitored.

The delay time of the device depended on two factors. For a lower gas concentration, the delay time was longer, however, for a thinner device, the delay time was less.

Exposing a device of known thickness to various concentrations of NO_x over a given length of time, it was found that the higher the gas concentration, the greater the change in current. The best device to use was found to be 0.185μm thick (or of a similar magnitude), as it did not saturate too early when exposed to NO_x gas (as did the thinnest device), nor did it show too many irregular readings (as did the thickest spun device). All devices showed a suitable recovery when the gas was removed, providing evidence that the effect was due to surface interactions.

5.2 Suggestions for further work

This thesis was researched over a period of one year and during that time, several topics were touched on which could be investigated further. They are as follows:

(a) Carrying out more experiments to quantify whether polyaniline in NMP solution behaves as a Newtonian or a non-Newtonian fluid.

(b) Measuring values of the refractive index, extinction coefficient and permittivity of emeraldine-base polyaniline as mentioned in Chapter 3.

(c) Performing further gas sensing experiments on polyaniline devices to see exactly how many times they can perform, how well they reverse back once the NO_x gas is removed, and how repeated exposure to this gas effects the device.

(d) Finding the effect of exposing polyaniline devices to other gases, such as hydrogen sulphide and carbon monoxide and comparing these results to the results presented in this thesis.

(e) Analyse the gas sensing data in terms of the diffusion process.

(f) The effect the gold electrodes have on the gas sensing results (i.e. vary electrode dimensions like electrode finger height, finger length and number of fingers.

(g) The gas sensing results should be modelled in terms of a diffusion process.

Work is being carried out at Durham to develop a field effect transistor (FET), using information gathered from this work. A thin film of polyaniline (the gate), is spun onto the silicon wafer transistor. This is to be used as a gas sensor and will be tested to monitor its response when exposed to various gases. The final product will be finished once the tests are completed and everything is working alright.

References

[1] J. Bredas - 'The Polyanilines' in Proceedings of the Nobel Symposium on conjugated polymers and related materials, Oxford, (1992).

[2] A.P Monkman and P.Adams - Synthetic Metals **40**(1991),87-96.